microRNA-15b contributes to depression-like behavior in mice by affecting synaptic protein levels and function in the nucleus accumbens

Received for publication, November 23, 2019, and in revised form, March 20, 2020 Published, Papers in Press, March 24, 2020, DOI 10.1074/jbc.RA119.012047

Li Guo[‡§], Zhaoming Zhu[¶], Guangyan Wang[¶], Shan Cui[‡], Meng Shen[¶], Zhenhua Song[¶], and Jin-Hui Wang[‡§1]

From the [‡]Institute of Biophysics, Chinese Academy of Sciences, Beijing 100101, China, the [§]University of Chinese Academy of Sciences, Beijing 100049, China, and the [¶]School of Pharmacy, Qingdao University, Qingdao Shandong 266021, China

Edited by Karin Musier-Forsyth

Major depression is a prevalent affective disorder characterized by recurrent low mood. It presumably results from stress-induced deteriorations of molecular networks and synaptic functions in brain reward circuits of genetically-susceptible individuals through epigenetic processes. Epigenetic regulator microRNA-15b inhibits neuronal progenitor proliferation and is up-regulated in the medial prefrontal cortex of mice that demonstrate depression-like behavior, indicating the contribution of microRNA-15 to major depression. Using a mouse model of major depression induced by chronic unpredictable mild stress (CUMS), here we examined the effects of microRNA-15b on synapses and synaptic proteins in the nucleus accumbens of these mice. The application of a microRNA-15b antagomir into the nucleus accumbens significantly reduced the incidence of CUMS-induced depression and reversed the attenuations of excitatory synapse and syntaxin-binding protein 3 (STXBP3A)/vesicle-associated protein 1 (VAMP1) expression. In contrast, the injection of a microRNA-15b analog into the nucleus accumbens induced depression-like behavior as well as attenuated excitatory synapses and STXBP3A/VAMP1 expression similar to the down-regulation of these processes induced by the CUMS. We conclude that microRNA-15b-5p may play a critical role in chronic stress-induced depression by decreasing synaptic proteins, innervations, and activities in the nucleus accumbens. We propose that the treatment of anti-microRNA-15b-5p may convert stress-induced depression into resilience.

Major depression is a low-mood disorder, in which patients show recurrent anhedonia, interest loss, and low self-esteem. The interaction between chronic stress and genetic susceptibility is presumably its etiology (1–5). Chronic stress that leads to negative emotional outcomes in genetically-susceptible individuals may dysfunction their neurons in the reward neural circuit, such as the ventral tegmental area, nucleus accumbens, and prefrontal cortex (6–13). However, most people do not suffer from depression in response to chronic stress, *i.e.* resilience (14). The elucidation of endogenous mechanisms underlying major depression *versus* resilience should shed light on developing therapeutic strategies to convert depression into resilience. Recently, the epigenetic process is thought to be a key switch from chronic stress to cellular and molecular pathology of major depression and resilience, especially microRNA (15–28). As microRNA interacts with mRNA, by which the binding of microRNAs with their dicers degrade mRNAs and weaken their translation (29–32), the role of microRNAs in major depression and resilience is based presumably on their influence on the expression levels of cell proteins. These molecular and cellular targets acted on by microRNAs for major depression *versus* resilience remain to be addressed.

The nucleus accumbens has been placed in the category of reward neural circuits (33–38), which regulates emotional reactions and cognitive processes (36, 39–41). For instance, structural elements and functional activities in neural circuits that include the nucleus accumbens are involved in the regulation of reward and fear memory (37, 42–47). Pathologically, some cell functions and signaling molecules in the nucleus accumbens are impaired in affective disorders (25, 38, 40, 48–52). The dysfunction of GABAergic neurons in the nucleus accumbens is relevant to major depression (51, 52, 54, 55). GABAergic synaptic transmission in the nucleus accumbens is deteriorated in depression-like mice, compared with resilience mice (55). These results indicate that GABAergic synapses and neurons in the nucleus accumbens may be cellular targets in major depression. In terms of molecular triggers, amygdala microRNA-15a is involved in the chronic stress (56). microRNA-15b has been found to inhibit neuronal progenitor proliferation (57) and to be up-regulated in the medial prefrontal cortex of depression-like mice by acting on synapse-relevant proteins (22). These results indicate that microRNA-15 may be an initiator of molecular and cellular changes in major depression. In this study, we intend to examine how microRNA-15b in the nucleus accumbens works to be one of the essential epigenetic molecules that impair GABAergic neurons and lead to depressive disorder.

Strategies to reveal the essential role of microRNA-15b in major depression to chronic unpredicted mild stress (CUMS)[2]

This work was supported by National Key R&D Program of China Grant 2016YFC1307101 and Natural Science Foundation of China Grants 81971027, 81930033, and 81671071 (to J.-H. W.). The authors declare that they have no conflicts of interest with the contents of this article.

[1] To whom correspondence should be addressed. Tel.: 86-86-10-64888472; E-mail: wangjinhui@ucas.ac.cn.

[2] The abbreviations used are: CUMS, chronic unpredictable mild stress; AAV, adeno-associated virus; FST, forced swimming test; NAc, nucleus accumbens; qPCR, quantitative polymerase chain reaction; sEPSC, spontaneous excitatory postsynaptic current; STXBP3A, syntaxin-binding protein 3; VAMP1, vesicle-associated membrane protein 1; YMT, Y-maze test; SPT, sucrose preference test; ANOVA, analysis of variance; CP, cumulative probability; ACSF, artificial cerebrospinal fluid; GABA, γ-aminobutyric acid; mPFC, medial prefrontal cortex.

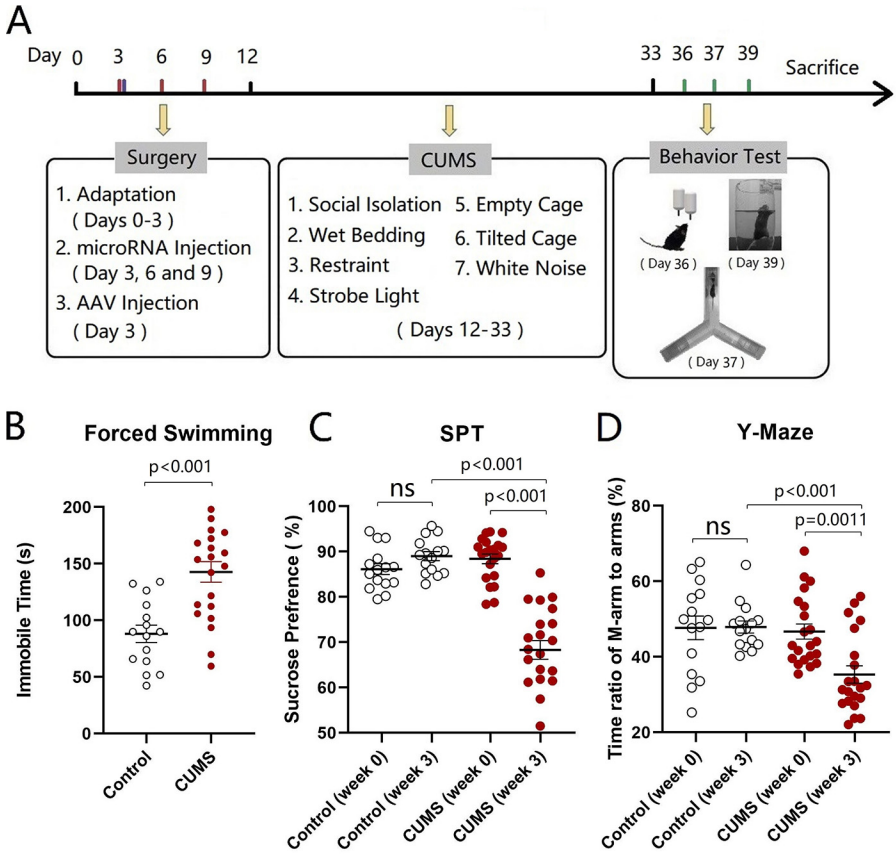

Figure 1. CUMS leads the mice to express depression-like behavior. *A* shows the procedures produced depression-like mice, including the adaptation for 1 week, the CUMS for 3 weeks, and the behavioral tests for 6 days. *B* illustrates immobile time of staying in the water cylinder in the FST from control mice (*open symbols*, $n = 15$) and CUMS-treated mice (*red symbols*, $n = 21$). *C* shows the SPT values (%) from control mice (*open symbols*, $n = 15$) and CUMS-treated mice (*red symbols*, $n = 21$). *D* illustrates the ratios of stay time in the M-arm to stay time in three arms by the YMT from control mice (*open symbols*, $n = 15$) and CUMS-treated mice (*red symbols*, $n = 21$). One-way ANOVA was used for statistical comparisons between control mice and CUMS-treated mice. Paired *t* test was used for statistical comparisons before and after the CUMS. *ns*, no statistical significance.

as well as its molecular and cellular targets in the nucleus accumbens are presented below. The tests of sucrose preference, Y-maze and forced swimming, were used to identify CUMS-induced depression-like behavior. Anti-microRNA-15b was done by microinjecting microRNA-15b antagomir into the nucleus accumbens. The effect of microRNA-15b was mimicked by microinjecting microRNA-15b agomir into this area. Synapse activities in the nucleus accumbens were monitored by electrophysiological whole-cell recordings in brain slices. Axon projections and synapse innervations were analyzed by neural tracing with AAV-conjugated fluorescent proteins. The molecular targets of microRNA-15b were identified by quantitative RT-PCR, Western blotting, and dual-luciferase reporter assay.

Results

Chronic unpredictable mild stress leads to depression-like behavior and GABAergic down-regulation in mice

After a week's accommodation, two groups of mice were placed into the control house and the house with CUMS for 3 weeks, respectively. Their mood state was assessed by the sucrose preference test (SPT), Y-maze test (YMT), and forced swimming test (FST). Compared with control mice, the mice in the CUMS house had an increased immobile time in the FST, a decreased sucrose preference, and a decreased M-arm stay time in the Y-arm maze. Values for immobile time are 142.8 ± 9.14 s in CUMS-treated mice (*red symbols* in Fig. 1*B*, $n = 21$) and 88.05 ± 7.7 s in control mice (*open symbols*; $n = 15$, $p < 0.001$, one-way ANOVA). SPT values in CUMS-treated mice are 68.31 ± 2.1% after the CUMS (*red symbols* in Fig. 1*C*) and 88.42 ± 1.06% before the CUMS (*red symbols*; $n = 21$, $p < 0.001$, paired *t* test). The ratios of the stay time in the M-arm to the stay time in total arms in CUMS-treated mice are 35.33 ± 2.29% after the CUMS (*red symbols* in Fig. 1*D*) and 46.72 ± 2.02% before the CUMS (*red symbols*; $n = 21$, $p < 0.01$, paired *t* test). Therefore, the CUMS induces the decreases in sucrose preference and social interaction as well as an increase of immobility in the forced swim, *i.e.* depression-like behavior in mice. We then examined cellular and molecular changes in the nucleus accumbens.

Excitatory synaptic transmission was studied at GABAergic neurons in the nucleus accumbens included in the coronal section of brain slices. Spontaneous excitatory postsynaptic currents (sEPSC) were recorded under the whole-cell voltage-clamp. sEPSC amplitudes and frequencies appear to be decreased on GABAergic neurons from CUMS-induced depression mice, compared with control mice (Fig. 2*A*). Fig. 2*B* illustrates the cumulative probabilities of sEPSC amplitudes in the CUMS-induced depression group (*red symbols*, $n = 14$ cells from five mice) and in the control group (*open symbols*, $n = 15$ cells from five mice). Fig. 2*B*, *inset*, shows that sEPSC ampli-

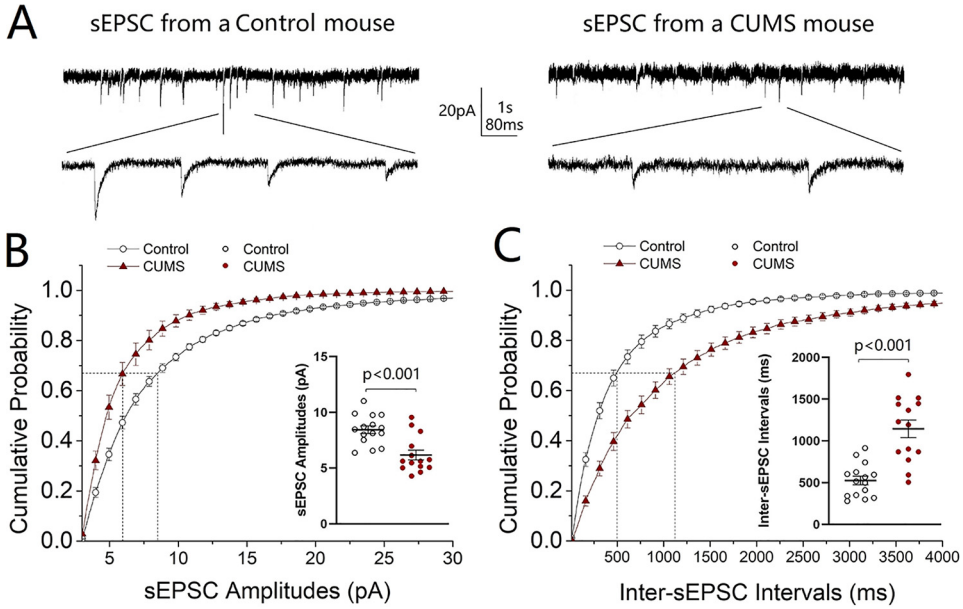

Figure 2. Excitatory synaptic transmission is down-regulated in GABAergic neurons of the nucleus accumbens from CUMS-induced depression-like mice. sEPSCs were recorded under voltage-clamp in the brain slices in the presence of 10 μM bicuculline. *A* shows sEPSCs from a control mouse (*left traces*) and a CUMS-induced depression mouse (*right traces*). Calibration symbols: *vertical*, 20 pA; *horizontal*, 1 s (*top*) and 80 ms (*bottom*). *B* shows cumulative probability *versus* sEPSC amplitudes from control group (*open symbols*, $n = 15$ cells from five mice) and CUMS-induced depression group (*red symbols*, $n = 14$ cells from five mice). *Dashed lines* indicate sEPSC amplitudes at cumulative probability to 67% (CP_{67}). The *inset* shows a comparison of sEPSC amplitudes at CP_{67} from control mice (*open symbols*) and CUMS-induced depression mice (*red symbols*). *C* shows cumulative probability *versus* inter-sEPSC intervals from control group (*open symbols*, $n = 15$ cells from five mice) and CUMS-induced depression group (*red symbols*, $n = 14$ cells from five mice). *Dashed lines* indicate the sEPSC interval at CP_{67}. The *inset* shows a comparison of sEPSC intervals at CP_{67} from control mice (*open symbols*) and CUMS-induced depression mice (*red symbols*). One-way ANOVA was used for statistical comparisons between control mice and CUMS-induced depression-like mice.

tudes at 67% cumulative probability are 8.43 ± 0.34 pA in control mice and 6.17 ± 0.44 pA in the CUMS-induced depression mice ($p < 0.001$). Fig. 2*C* shows the cumulative probabilities of inter-sEPSC intervals in the CUMS-induced depression group (*red symbols*, $n = 14$ from five mice) and in the control group (*open symbols*, $n = 15$ cells from five mice). Fig. 2*C*, *inset*, shows that inter-sEPSC intervals at 67% cumulative probability are 526 ± 51.20 ms in the control mice and 1144 ± 104.7 ms in the CUMS-induced depression mice ($p < 0.001$). The decreased sEPSC amplitude and frequency indicate that excitatory synapses on GABAergic neurons in the nucleus accumbens are deteriorated in the CUMS-induced depression mice.

Excitatory synapse innervation from the medial prefrontal cortex to neurons in the nucleus accumbens was analyzed in the CUMS-induced depression mice and the control mice. GABAergic neurons in mouse brain were genetically labeled by green fluorescent protein (GFP). mCherry carried by adeno-associated viruses (AAV) was injected into the medial prefrontal cortex (see under "Experimental procedures" for details). Subsequently, these mice were placed in either a CUMS house or a control house for 3 weeks. The contacts (yellow) between presynaptic axonal boutons (red) from the medial prefrontal cortex and postsynaptic GABAergic neurons (green) in the nucleus accumbens were counted to be synapse innervations. As shown in Fig. 3, *A* and *B*, excitatory synapse innervations on GABAergic neurons are lower in the CUMS-induced depression mice than in controls. The numbers of boutons on GABAergic neurons are 12.67 ± 0.64 per cell in the control group (*open symbols* in Fig. 3*C*; $n = 27$ cells from five mice) and 9.57 ± 0.4 per cell in the CUMS-induced depression group (*red*

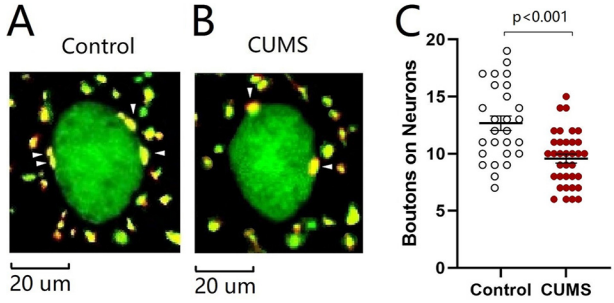

Figure 3. Excitatory synapse innervations from the mPFC to GABAergic neurons in the NAc are lowered in the CUMS-induced depression-like mice. *A* and *B* illustrate innervations (*yellow*) from mPFC to GABAergic neurons (*green*) of NAc in control mice (*A*) and CUMS-induced depression mice (*B*). *C* shows the innervations from mPFC to GABAergic neurons of NAc in the control group (*open symbols*, $n = 27$ cells from five mice) and CUMS-induced depression group (*red symbols*, $n = 35$ cells from five mice). One-way ANOVA was used for statistical comparisons between control mice and CUMS-induced depression-like mice. *Arrowheads* indicate synaptic contacts between presynaptic boutons and GABAergic cell bodies.

symbols; $n = 35$ cells from five mice; $p < 0.001$, one-way ANOVA). This result indicates that excitatory synapse innervation to GABAergic neurons in the nucleus accumbens from the medial prefrontal cortex is lowered in the CUMS-induced depression mice.

To the functional and morphological down-regulations of excitatory synapses onto GABAergic neurons, we assumed that the expression of genes and proteins relevant to synapse structure and function was attenuated. Genes *VAMP1* and *STXBP3A* that encode vesicle-associated membrane protein and syntaxin-binding protein (58–61) were selected to examine the molecular basis of synapse down-regulation. The reason for examining the changes of presynaptic targets is based on the

results above that presynaptic transmitter release and synapse innervations onto nucleus accumbens neurons are lowered in the CUMS-induced depression. Their mRNAs were analyzed by quantitative RT-PCR, which were harvested from tissues of the nucleus accumbens in the CUMS-induced depression mice and controls. The expression level of *VAMP1* decreases from 100.16 ± 2.01% in control mice (*open symbols* in Fig. 4*A*, $n = 6$) to 41.60 ± 6.42% in the CUMS-induced depression mice (*red symbols*; $n = 6$, $p < 0.001$, one-way ANOVA). The expression level of *STXBP3A* attenuates from 100.1 ± 1.62% in control mice (*open symbols* in Fig. 4*B*, $n = 6$) to 55.98 ± 5.24% in the CUMS-induced depression mice (*red symbols*; $n = 6$, $p < 0.001$, one-way ANOVA). In addition, proteins VAMP1 and STXBP3A were investigated by Western blotting, which were harvested from tissues of the nucleus accumbens from CUMS-induced depression mice and controls. The level of VAMP1 decreases from 100.0 ± 8.22% in control mice (*open symbols* in Fig. 4*D*, $n = 6$) to 28.65 ± 5.73% in the CUMS-induced depression mice (*red symbols*; $n = 6$, $p = 0.0021$, one-way ANOVA). The level of STXBP3A attenuates from 100.0 ± 4.81% in control mice (*open symbols* in Fig. 4*E*, $n = 6$) to 52.72 ± 8.04% in CUMS depression-like mice (*red symbols*; $n = 6$, $p = 0.0072$, one-way ANOVA). Based on the quantitative analyses of mRNA and proteins, genes and proteins relevant to the fusion of synaptic vesicles with presynaptic membrane for transmitter release are down-regulated in the nucleus accumbens from CUMS-induced depression mice.

The results above indicate that the CUMS down-regulates synapse-relevant proteins (VAMP1 and STXBP3A), excitatory synapse innervations, and synaptic transmission in the nucleus accumbens, which in turn induces major depression. This indication needs to be validated. The initiative factor from the CUMS to molecular and cellular changes remains to be found. Previous studies indicate the involvement of microRNAs in major depression (15–19, 21, 23). mRNA and microRNA interact with each other, by which the binding of microRNA to dicers degrades mRNA to weaken mRNA translation (30, 31). microRNA-15b-5p is elevated in the CUMS-induced depression (22). microRNA-15b-5p directly acts to mRNAs *VAMP1* and *STXBP3A* (Fig. 5). We hypothesize that microRNA-15b-5p may be one of the CUMS-acted initiative factors that induce pathological alternations in synapse molecules, morphology, and functions. If this is the case, anti-microRNA-15b-5p is expected to rescue the down-regulations of synapse-related proteins and synapses in the nucleus accumbens of CUMS-induced depression mice, and microRNA-15b-5p derivatives should induce depression-like behavior and synapse-relevant changes.

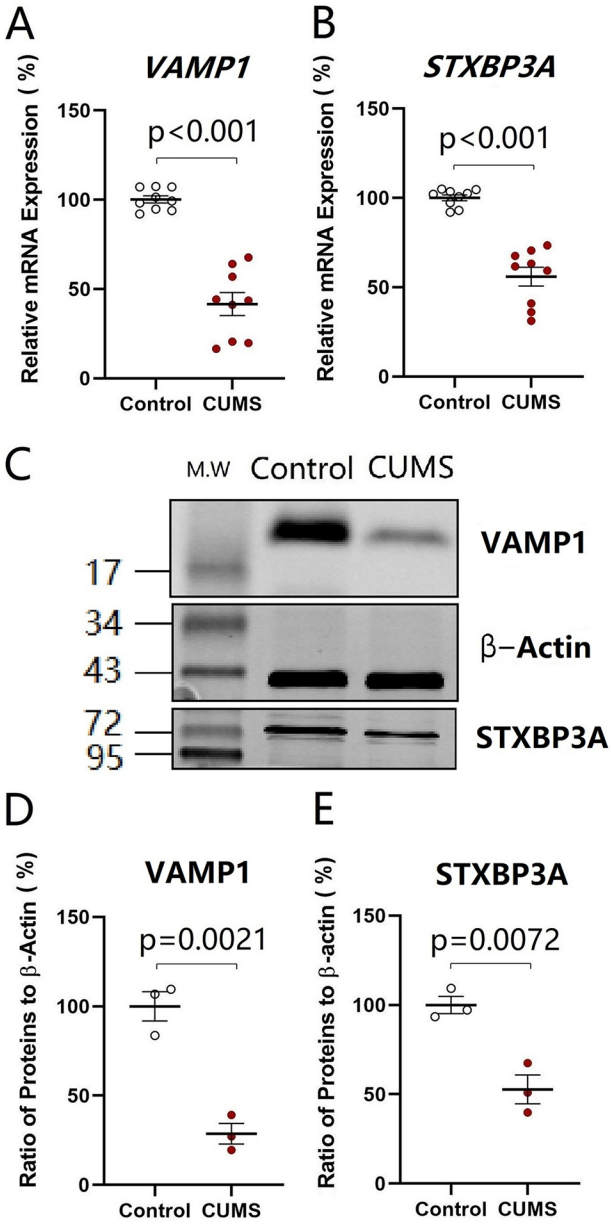

Figure 4. Genes and proteins in relevance to the fusion of synaptic vesicles with presynaptic membrane for releasing transmitters are down-regulated in the nucleus accumbens from CUMS-induced depression mice. The expressions of mRNA *VAMP1* and *STXBP3A* were analyzed by quantitative RT-PCR. The expressions of proteins VAMP1 and STXBP3A were measured by Western blotting. *A* and *B* show the relative value of mRNAs *VAMP1* (*A*) and *STXBP3A* (*B*) in control mice (*open symbols*, $n = 6$) and CUMS-induced depression mice (*red symbols*, $n = 6$), in which internal control is β-actin. *C* shows the expressions of VAMP1 and STXBP3A from control mice and CUMS-induced depression mice, in which the internal control is β-actin. *D* and *E* illustrate the normalized ratios of VAMP1 (*D*) and STXBP3A (*E*) to β-actin from control mice (*open symbols*, $n = 6$) and CUMS-induced depression mice (*red symbols*, $n = 6$). The relative ratios for control mice are normalized to be 1. One-way ANOVA was used for statistical comparisons between control mice and CUMS-induced depression-like mice.

Anti-microRNA-15b-5p significantly rescues CUMS-induced depression and synapse down-regulation

In addition to control and CUMS-treated mice, another two groups of mice added to our study received the microinjections of microRNA-15b-5p antagomir and microRNA-15b-5p antagomir-control into the nucleus accumbens, respectively. The reason for examining the role of microRNA15b is based on our previous studies that microRNA-15b is up-regulated in the medial prefrontal cortex from CUMS-induced depression mice (22, 62), and the change in presynaptic targets has been seen where presynaptic transmitter release and synapse innervations onto nucleus accumbens neurons from the medial prefrontal cortex are lowered in the CUMS-induced depression. These two groups of mice with microinjections were placed in the CUMS house for 3 weeks, similarly to CUMS-treatment

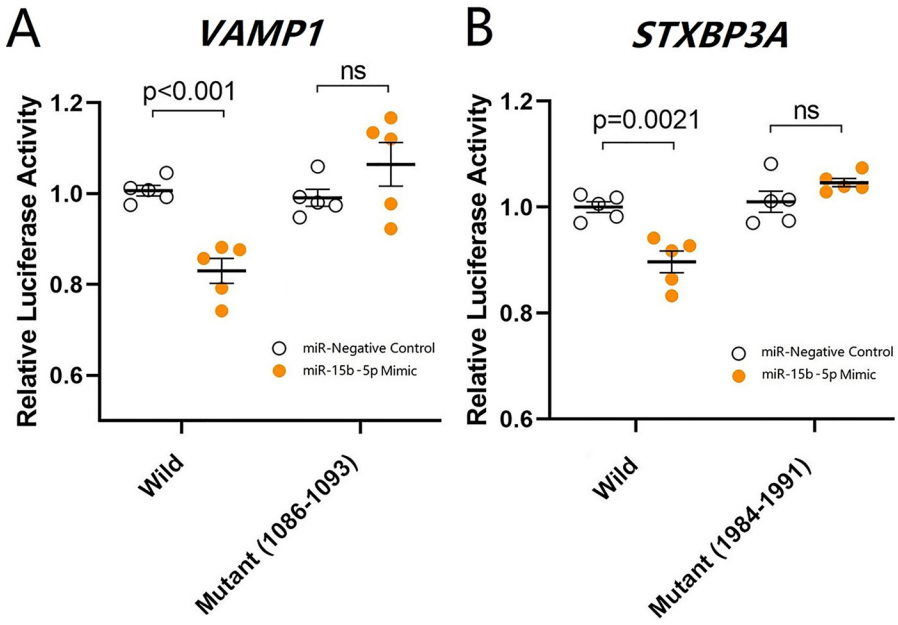

Figure 5. miR-15b-5p–targeted mRNAs for synaptic vesicle fusion-related proteins are validated by luciferase reporter assay. *A* and *B,* luciferase reporter assay is performed by the co-transfection of luciferase reporter containing the wildtype or mutant 3′-untranslated repeat (UTR) of VAMP1 and STXBP3A mRNA with miR-15b-5p mimic and negative control into HEK293T cells. Luciferase activity was determined 48 h after co-transfection. $p, < 0.01$, and $p, < 0.001$. *ns*, no statistical significance.

alone. Their mood state was assessed by SPT, YMT, and FST. Compared with controls, CUMS, and microRNA-15b-5p antagomir-control plus CUMS groups, mice that have received microRNA-15b-5p antagomir plus the CUMS demonstrated a significant improvement of CUMS-induced depression-like behavior. The values of immobile time in the FST are 88.05 ± 7.71 s in control mice (*open symbols* in Fig. 6*A*; $n = 15$), 142.8 ± 9.14 s in CUMS-treated mice (*red symbols*; $n = 21$), 150.5 ± 7.1 s in microRNA-15 antagomir-control plus CUMS mice (*circled dot symbols*; $n = 15$), and 111.8 ± 10.1 s in microRNA-15b-5p antagomir plus CUMS mice (*blue symbols*; $n = 18$, $p < 0.01$, one-way ANOVA). SPT values are 89.03 ± 1.00% in control mice (*open symbols* in Fig. 6*B*; $n = 15$), 68.31 ± 2.08% in CUMS-treated mice (*red symbols*; $n = 21$), 71.89 ± 2.50% in microRNA-15 antagomir-control plus CUMS mice (*circled dot symbols*; $n = 15$), and 82.26 ± 2.03% in microRNA-15b-5p antagomir plus CUMS mice (*blue symbols*; $n = 18$, p values are less than 0.001 to 0.05, one-way ANOVA). The ratios of stay time in the M-arm to stay time in total arms are 47.92 ± 1.59% in control mice (*open symbols* in Fig. 6*C*; $n = 15$), 35.33 ± 2.29% in CUMS-treated mice (*red symbols*; $n = 21$), 34.13 ± 1.43% in microRNA-15b-5p antagomir-control plus CUMS mice (*circled dot symbols*; $n = 15$), and 44.37 ± 3.21% in microRNA-15b-5p antagomir plus CUMS mice (*blue symbols*; $n = 18$, p values are less than 0.001 to 0.05, one-way ANOVA). This result indicates that anti-microRNA-15b-5p in the nucleus accumbens significantly rescues CUMS-induced depression-like behavior. We subsequently examined cellular and molecular mechanisms underlying this rescue.

The influence of microRNA-15b-5p down-regulation on cell functions was examined by recording sEPSCs on GABAergic neurons in the nucleus accumbens from control mice, CUMS-induced depression mice, and microRNA-15b-5p antagomir-injection plus CUMS-treatment mice. microRNA-15b-5p antagomir in the nucleus accumbens appears to rescue the decrease of excitatory synaptic transmission induced by the CUMS (Fig. 7*A*). Fig. 7*B* illustrates the cumulative probability of sEPSC amplitudes in the control group (*open symbols*; $n = 15$ cells from five mice), CUMS-induced depression group (*red symbols*, $n = 14$ cells from five mice), and microRNA-15b-5p antagomir-injection plus CUMS group (*blue symbols*, $n = 14$ cells from five mice). Fig. 7*B*, *inset*, illustrates that sEPSC amplitudes at 67% cumulative probability are 8.43 ± 0.34 pA in control mice (*open symbols*), 6.17 ± 0.44 pA in the CUMS-induced depression mice (*red symbols*), and 7.32 ± 0.34 pA in microRNA-15b-5p antagomir-injection plus CUMS-treated mice (*blue symbols*; $p < 0.001$ and 0.05, respectively). Fig. 7*C* shows the cumulative probability of inter-EPSC intervals in the control group (*open symbols*; $n = 15$ cells from five mice), CUMS-induced depression group (*red symbols*, $n = 14$ cells from five mice), and microRNA-15b-5p antagomir-injection plus CUMS group (*blue symbol*, $n = 14$ cells from five mice). Fig. 7*C*, *inset*, shows that inter-sEPSC intervals at 67% cumulative probability are 526 ± 51.2 ms in control mice (*open symbols*), 1144 ± 104.7 ms in the CUMS-induced depression mice (*red symbols*), and 729.8 ± 70.4 ms in microRNA-15b-5p antagomir-injection plus CUMS-treated mice (*blue symbols*, p values are less than 0.001 to 0.05). The CUMS-induced down-regulation of excitatory synaptic transmission on GABAergic neurons in the nucleus accumbens is reversed by anti-microRNA-15b-5p. Thus, microRNA-15b-5p is required for the down-regulation of synaptic transmission in the CUMS-induced depression.

The influence of microRNA-15b-5p down-regulation on synapse innervations was studied by neural tracing in the nucleus accumbens from control mice, CUMS-induced depression mice, and microRNA-15b-5p antagomir-injection plus CUMS-treated mice. AAV-carried mCherry was injected and

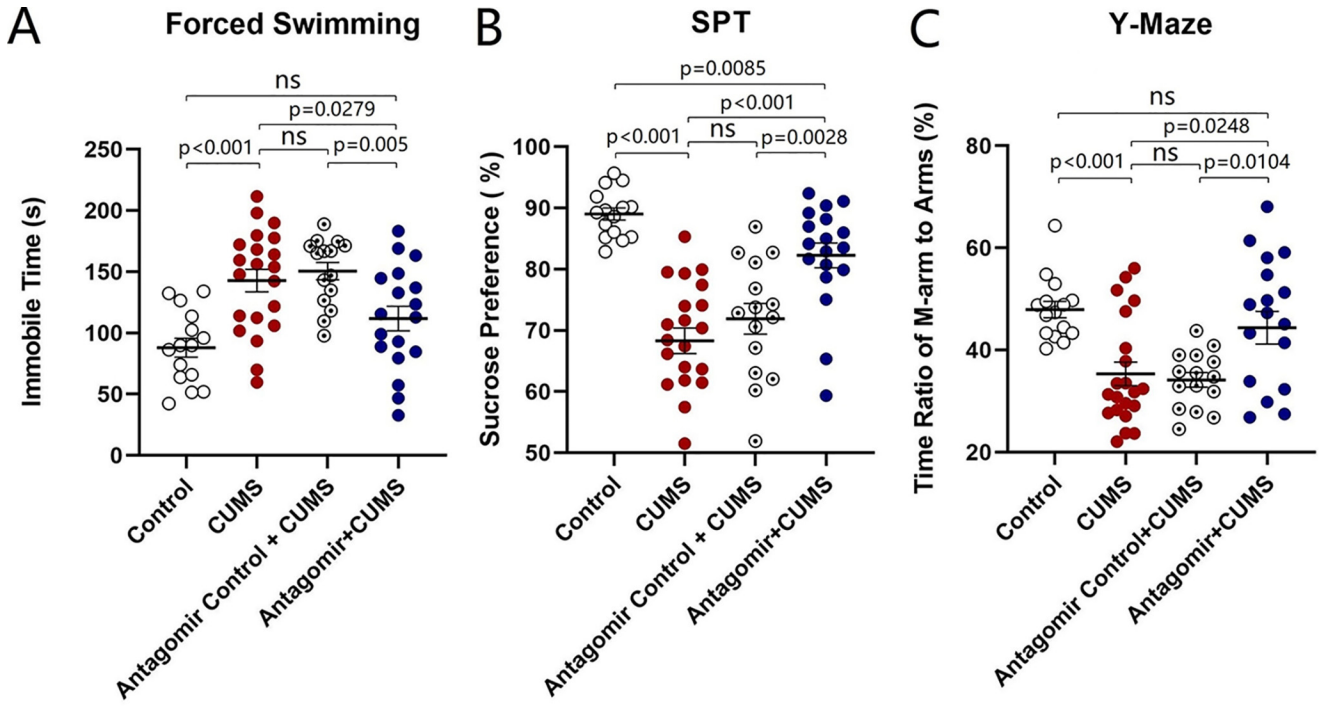

Figure 6. Anti-microRNA-15b-5p rescues CUMS-induced depression-like behavior. *A* illustrates immobile time in the forced swim test from control mice (*open symbols*, $n = 15$), CUMS-induced depression mice (*red symbols*, $n = 21$), microRNA-15b-5p antagomir-control plus CUMS mice (*circled dot symbols*, $n = 15$), and microRNA-15b-5p antagomir-injection plus CUMS mice (*blue symbols*, $n = 18$). *B* shows values of the sucrose preference test (%) in control mice (*open symbols*, $n = 15$), CUMS-induced depression mice (*red symbols*, $n = 21$), microRNA-15b-5p antagomir-control plus CUMS mice (*circled dot symbols*, $n = 15$), and microRNA-15b-5p antagomir-injection plus CUMS mice (*blue symbols*, $n = 18$). *C* illustrates the ratios of stay time in M-arm to stay time in three arms by the Y-maze test from control mice (*open symbols*, $n = 15$), CUMS-induced depression mice (*red symbols*, $n = 21$), microRNA-15b-5p antagomir-control plus CUMS mice (*circled dot symbols*, $n = 15$), and microRNA-15b-5p antagomir-injection plus CUMS mice (*blue symbols*, $n = 18$). One-way ANOVA was used for statistical comparisons among control mice, CUMS-induced depression mice, microRNA-15b-5p antagomir-control plus CUMS mice, and microRNA-15b-5p antagomir-injection plus CUMS mice. *ns*, no statistical significance.

expressed in the medial prefrontal cortex. microRNA-15b-5p antagomir was injected into the nucleus accumbens. After various treatments, their mood state was assessed by SPT, YMT, and FST. mCherry-labeled axon boutons onto GABAergic neurons were analyzed in the nucleus accumbens by scanning slice sections under a confocal microscope. microRNA-15b-5p antagomir appears to reverse the decrease of synapse innervation from the medial prefrontal cortex to GABAergic neurons in the nucleus accumbens induced by the CUMS (Fig. 8, *A–C*). Fig. 8*D* illustrates that boutons per GABAergic neuron are 12.67 ± 0.64 in the control group (*open symbols*; $n = 27$ cells from five mice), 9.57 ± 0.40 in the CUMS-induced depression group (*red symbols*, $n = 35$ cells from five mice), and 11.70 ± 0.47 in microRNA-15b-5p antagomir-injection plus CUMS group (*blue symbols*, $n = 30$ cells from five mice, $p < 0.01$, one-way ANOVA). The CUMS-induced decrease of excitatory synapse innervations onto GABAergic neurons in the nucleus accumbens is reversed by anti-microRNA-15b-5p. In other words, microRNA-15b-5p is required for the down-regulation of synapse innervations in the CUMS-induced depression.

The effect of microRNA-15b-5p down-regulation on synapse-relevant genes *VAMP1* and *STXBP3A* was tested by quantitative RT-PCR in the nucleus accumbens from control mice, CUMS-induced depression mice, and microRNA-15b-5p antagomir-injection plus CUMS-treated mice. microRNA-15b-5p antagomir was injected into the nucleus accumbens. After various treatments, their mood was assessed by SPT, YMT, and FST. The tissues of the nucleus accumbens were harvested from these mice for qRT-PCR. The expression of *VAMP1* decreases from 100.16 ± 2.01% in control mice (*open symbols* in Fig. 9*A*; $n = 6$) to 41.60 ± 6.42% in the CUMS-induced depression mice (*red symbols*; $n = 6$), which is reversed to 67.25 ± 5.19% in microRNA-15b-5p antagomir-injection plus CUMS-treated mice (*blue symbols*; $n = 6$, $p < 0.01$, one-way ANOVA). The expression of *STXBP3A* attenuates from 100.1 ± 1.62% in control mice (*open symbols* in Fig. 9*B*; $n = 6$) to 55.98 ± 5.24% in the CUMS-induced depression mice (*red symbols*, $n = 6$), which is reversed to 73.93 ± 4.83% in microRNA-15b-5p antagomir-injection plus CUMS-treated mice (*blue symbols*; $n = 6$, $p < 0.05$, one-way ANOVA). The CUMS-induced decrease of synapse-relevant genes *VAMP1* and *STXBP3A* in the nucleus accumbens is significantly but partially reversed by anti-microRNA-15b-5p.

The effect of microRNA-15b-5p down-regulation on synapse-relevant proteins VAMP1 and STXBP3A was tested by Western blotting in the nucleus accumbens from control mice, CUMS-induced depression mice, and microRNA-15b-5p antagomir-injection plus CUMS-treated mice. microRNA-15b-5p antagomir was injected into the nucleus accumbens. The tissues of the nucleus accumbens were harvested from these mice for Western blotting. As illustrated in Fig. 9*C*, microRNA-15b-5p antagomir appears to reverse the decrease of VAMP1 and STXBP3A in the nucleus accumbens induced

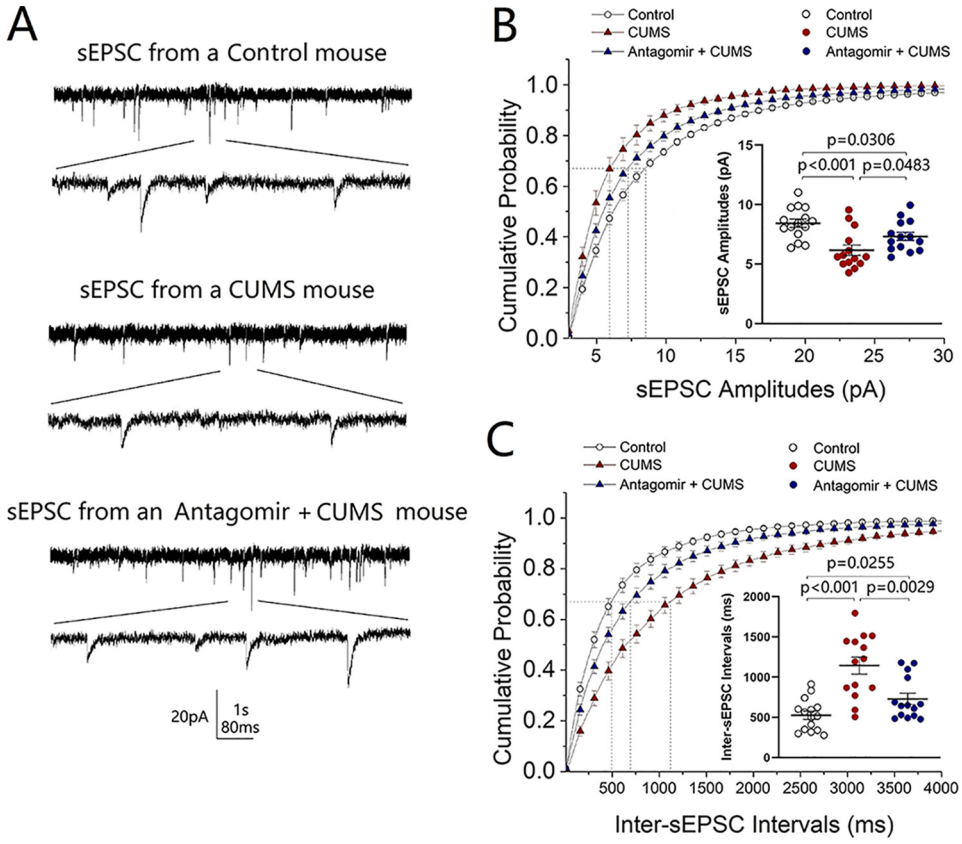

Figure 7. Anti-microRNA-15b-5p rescues excitatory synaptic transmission in GABAergic neurons of the nucleus accumbens impaired by CUMS. sEPSCs were recorded under voltage-clamp in the brain slices in the presence of 10 μM bicuculline. *A* shows sEPSCs from a control mouse (*top traces*), a CUMS-induced depression mouse (*middle traces*), and a microRNA-15b-5p antagomir-injection plus CUMS mouse (*bottom traces*). Calibration symbols: *vertical*, 20 pA; *horizontal*, second (*top*) and 80 ms (*bottom*) in *horizontal*. *B* shows cumulative probability *versus* sEPSC amplitudes from control group (*open symbols*, n = 15 cells from five mice), CUMS-induced depression group (*red symbols*, n = 14 cells from five mice), and microRNA-15b-5p antagomir-injection plus CUMS group (*blue symbols*, n = 14 cells from five mice). *Dashed lines* indicate sEPSC amplitudes at CP67. The *inset* shows a comparison of sEPSC amplitudes at CP67 from control mice (*open symbols*), CUMS-induced depression mice (*red symbols*), and microRNA-15b-5p antagomir-injection plus CUMS mice (*blue symbols*). *C* shows cumulative probability *versus* inter-sEPSC intervals from control group (*open symbols*, n = 15 cells from five mice), CUMS-induced depression group (*red symbols*, n = 14 cells from five mice), and microRNA-15b-5p antagomir injection plus CUMS group (*blue symbols*, n = 14 cells from five mice). *Dashed lines* indicate sEPSC intervals at CP67. The *inset* shows a comparison of sEPSC intervals at CP67 from control mice (*open symbols*), CUMS-induced depression-like mice (*red symbols*), and microRNA-15b-5p antagomir-injection plus CUMS mice (*blue symbols*). One-way ANOVA was used for statistical comparisons among control mice, CUMS-induced depression mice, and microRNA-15b-5p antagomir-injection plus CUMS mice.

by the CUMS. The expression of VAMP1 decreases from 100 ± 8.22% in control mice (*open symbols* in Fig. 9*D*; n = 6) to 28.65 ± 5.73% in the CUMS-induced depression mice (*red symbols*, n = 6), which is reversed to 63.43 ± 8.48% in microRNA-15b-5p antagomir-injection plus CUMS-treated mice (*blue symbols*; n = 6, $p < 0.05$, one-way ANOVA). The expression of STXBP3A changes from 100.0 ± 4.81% in control mice (*open symbols* in Fig. 9*E*; n = 6) to 52.7 ± 8% in the CUMS-induced depression mice (*red symbols*, n = 6), which is reversed to 88.12 ± 6.3% in microRNA-15b-5p antagomir-injection plus CUMS-treated mice (*blue symbols*; n = 6, $p < 0.05$, one-way ANOVA). The CUMS-induced decrease of synapse-relevant proteins VAMP1 and STXBP3A in the nucleus accumbens is significantly but partially reversed by anti-microRNA-15b-5p. In summary, microRNA-15b-5p is required for the down-regulation of genes and proteins (VAMP1 and STXBP3A) in the CUMS-induced depression.

microRNA-15b-5p agomir mimics CUMS-induced depression and synapse down-regulation

In addition to control and CUMS-treatment groups, other two groups of mice were taken into our study that received microinjections of microRNA-15b-5p agomir and microRNA-15b-5p agomir-control into the nucleus accumbens, respectively. The mice with microinjections were placed in the control house for 3 weeks. Their mood was assessed by SPT, YMT, and FST. The values of immobile time in the FST are 88.05 ± 7.71 s in control mice (*open symbols* in Fig. 10*A*; n = 15), 142.8 ± 9.14 s in CUMS-treated mice (*red symbols*; n = 21), 92.36 ± 9.10 s in microRNA-15 agomir-control mice (*circled* × *symbols*; n = 15), and 130.2 ± 8.81 s in microRNA-15b-5p agomir-injection mice (*yellow symbols*; n = 20, $p < 0.01$, one-way ANOVA). SPT values are 89.03 ± 1.00% in control mice (*open symbols* in Fig. 10*B*; n = 15), 68.31 ± 2.08% in CUMS-treated mice (*red symbols*; n = 21), 90.76 ± 0.89% in microRNA-15b-5p agomir-control mice (*circled* × *symbols*; n = 15), and 72.66 ± 2.37% in microRNA-15b-5p agomir-injection mice (*yellow symbols*; n = 20, p values are less than 0.001 to 0.05, one-way ANOVA). The ratios of stay time in the M-arm to stay time in total arms are 47.92 ± 1.59% in control mice (*open symbols* in Fig. 10*C*; n = 15), 35.33 ± 2.3% in CUMS-treated mice (*red symbols*; n = 21), 45.32 ± 2.28% in microRNA-15b-5p agomir-control mice (*circled* × *symbols*; n = 15), and 32.53 ± 3.09% in

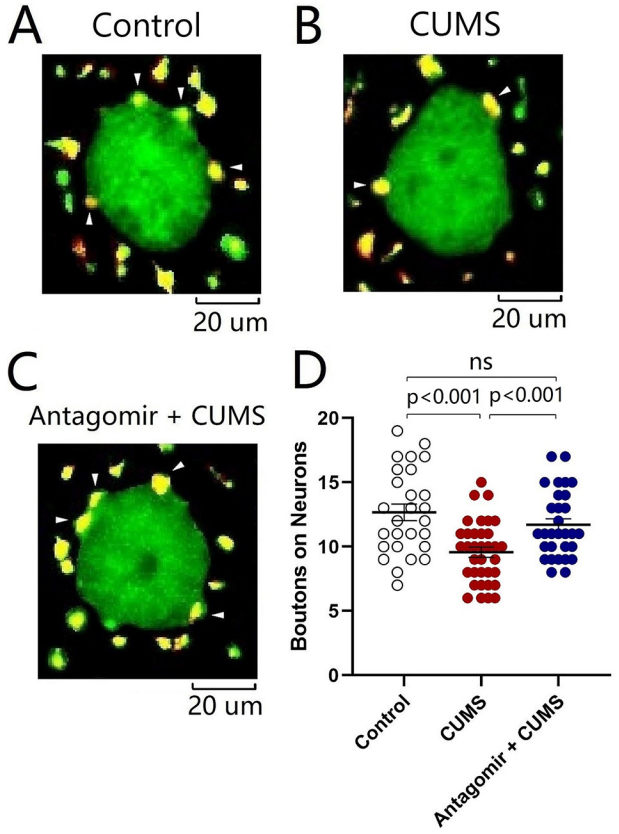

Figure 8. Decrease of synapse innervations from the mPFC to GABAergic neurons in the NAc is rescued by anti-microRNA-15b-5p. *A–C* illustrate the innervations (*yellow*) from mPFC to GABAergic neurons (*green*) of the NAc in control mice (*A*), CUMS-induced depression-like mice (*B*), and microRNA-15b-5p antagomir-injection plus CUMS mice (*C*). *D* shows the innervations from mPFC to GABAergic neurons of NAc from control group (*open symbols*, $n = 27$ cells from five mice), CUMS-induced depression group mice (*red symbols*, $n = 35$ cells from five mice), and microRNA-15b-5p antagomir-injection plus CUMS group (*blue symbols*, $n = 30$ cells from five mice). One-way ANOVA was used for statistical comparisons among control mice, CUMS-induced depression mice, and microRNA-15b-5p antagomir-injection plus CUMS mice. *Arrowheads* indicate synaptic contacts between presynaptic boutons and GABAergic cell bodies. *ns*, no statistical significance.

microRNA-15b-5p agomir-injection mice (*yellow symbols*; $n = 20$, p values are less than 0.001 to 0.05, one-way ANOVA). This result indicates that microRNA-15b-5p in the nucleus accumbens leads to depression-like behavior similarly to those induced by the CUMS. We also studied cellular and molecular mechanisms underlying this mimic.

The influence of microRNA-15b-5p up-regulation on cellular function was examined by recording sEPSCs on GABAergic neurons in the nucleus accumbens from control mice, CUMS-induced depression mice, and microRNA-15b-5p agomir-injection mice. microRNA-15b-5p agomir in the nucleus accumbens appears to lower excitatory synaptic transmission similarly to those by the CUMS (Fig. 11*A*). Fig. 11*B* shows the cumulative probability of sEPSC amplitudes in the control group (*open symbols*; $n = 15$ cells from five mice), CUMS-induced depression group (*red symbols*, $n = 14$ cells from five mice), and microRNA-15b-5p agomir-injection group (*yellow symbols*, $n = 12$ cells from five mice). Fig. 11*B*, *inset*, shows that sEPSC amplitudes at 67% cumulative probability are 8.43 ± 0.34 pA in control mice (*open symbols*), 6.17 ± 0.44 pA in the

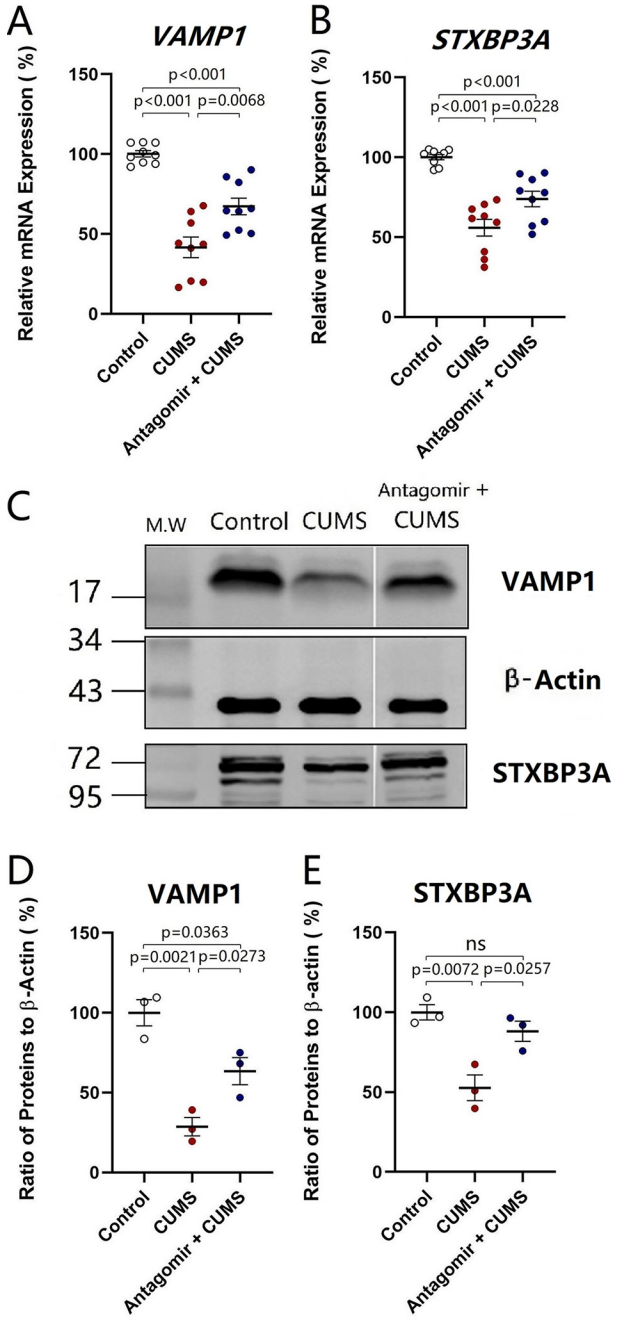

Figure 9. Anti-microRNA-15b-5p rescues the decrease of VAMP1 and STXBP3A in the NAc induced by the CUMS. The expressions of mRNAs *VAMP1* and *STXBP3A* were analyzed by quantitative RT-PCR. The expression of proteins VAMP1 and STXBP3A were measured by Western blotting. *A* and *B* show the relative value of mRNA for *VAMP1* (*A*) and *STXBP3A* (*B*) in control mice (*open symbols*, $n = 6$), CUMS-induced depression mice (*red symbols*, $n = 6$), and microRNA-15b-5p antagomir-injection plus CUMS mice (*blue symbols*, $n = 6$), in which internal control is β-actin. *C* shows the expressions of VAMP1 and STXBP3A from control mice, CUMS-induced depression mice, and microRNA-15b-5p antagomir-injection plus CUMS mice, in which internal control is β-actin. *D* and *E* show the normalized ratios of VAMP1 (*D*) and STXBP3A (*E*) expression to β-actin from control mice (*open symbols*, $n = 6$), CUMS-induced depression mice (*red symbols*, $n = 6$), and microRNA-15b-5p antagomir-injection plus CUMS mice (*blue symbols*, $n = 6$). The relative ratios for control mice are normalized to be 1. One-way ANOVA was used for statistical comparisons among control mice, CUMS-induced depression-like mice, and microRNA-15b-5p antagomir-injection plus CUMS mice. *ns*, no statistical significance.

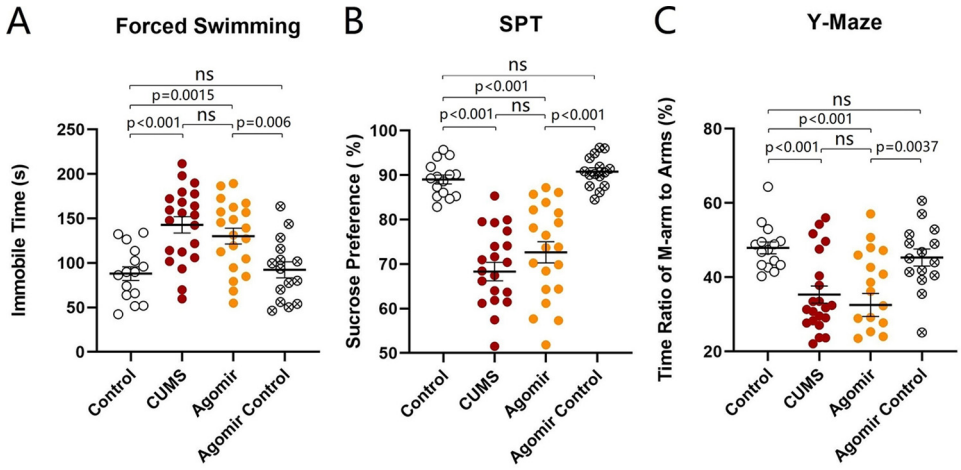

Figure 10. microRNA-15b-5p in the nucleus accumbens evokes depression-like behavior in mice similarly to those induced by the CUMS. *A* illustrates the immobile time in the FST from control mice (*open symbols*, $n = 15$), CUMS-induced depression mice (*red symbols*, $n = 21$), microRNA-15b-5p agomir-control mice (*circled* × *symbols*, $n = 15$), and microRNA-15b-5p agomir-injection mice (*yellow symbols*, $n = 20$). *B* shows the SPT values (%) from control mice (*open symbols*, $n = 15$), CUMS-induced depression mice (*red symbols*, $n = 21$), microRNA-15b-5p agomir-control mice (*circled* × *symbols*, $n = 15$), and microRNA-15b-5p agomir-injection mice (*yellow symbols*, $n = 20$). *C* illustrates the ratios of stay time in M-arm to stay time in three arms by the YMT from control mice (*open symbols*, $n = 15$), CUMS-induced depression mice (*red symbols*, $n = 21$), microRNA-15b-5p agomir-control mice (*circled* × *symbols*, $n = 15$), and microRNA-15b-5p agomir-injection mice (*yellow symbols*, $n = 20$). One-way ANOVA was used for statistical comparisons among control mice, CUMS-induced depression mice, microRNA-15b-5p agomir-control mice, and microRNA-15b-5p agomir-injection mice. *ns*, no statistical significance.

CUMS-induced depression mice (*red symbols*), and 6.69 ± 0.41 pA in microRNA-15b-5p agomir-injection mice (*yellow symbols*; $p < 0.01$). Fig. 11*C* illustrates the cumulative probability of inter-sEPSC intervals in the control group (*open symbols*; $n =$ 15 cells from five mice), CUMS-induced depression group (*red*, $n = 14$ cells from five mice), and microRNA-15b-5p agomir-injection group (*yellow*, $n = 12$ cells from five mice). Fig. 11*C*, *inset*, shows that inter-sEPSC intervals at 67% cumulative probability are 526 ± 51.2 ms in control mice (*open symbols*), 1144 ± 104.7 ms in the CUMS-induced depression mice (*red symbols*), and 1029 ± 87.63 ms in microRNA-15b-5p agomir-injection mice (*yellow symbols*, $p < 0.001$). The CUMS-induced decrease of excitatory synaptic transmission on GABAergic neurons in the nucleus accumbens is mimicked by microRNA-15b-5p derivatives. In other words, microRNA-15b-5p sufficiently induces the down-regulation of synaptic transmission similarly to that in the CUMS-induced depression.

The effect of microRNA-15b-5p up-regulation on synapse innervations was examined by neural tracing in the nucleus accumbens from control mice, CUMS-induced depression mice, and microRNA-15b-5p agomir-injection mice. AAV-carried mCherry was injected and expressed in the medial prefrontal cortex, and microRNA-15b-5p agomir was injected in the nucleus accumbens. After various treatments, their mood state was assessed by SPT, YMT, and FST. microRNA-15b-5p agomir appears to attenuate synapse innervations from the medial prefrontal cortex to GABAergic neurons in the nucleus accumbens similarly to that by the CUMS (Fig. 12, *A–C*). Fig. 12*D* shows that boutons per GABAergic neuron are 12.67 ± 0.64 in the control group (*open symbols*; $n = 27$ cells from five mice), 9.57 ± 0.40 in the CUMS-induced depression group (*red symbols*, $n = 35$ cells from five mice), and 9.03 ± 0.5 in microRNA-15b-5p agomir-injection group (*yellow symbols*; $n = 31$ cells from five mice, $p < 0.001$, one-way ANOVA). The CUMS-induced decrease of excitatory synapse innervations on GABAergic neurons in the nucleus accumbens is mimicked by microRNA-15b-5p derivates. In other words, microRNA-15b-5p sufficiently induces for the impairment of synapse innervations similarly to that in the CUMS-induced depression.

The influence of microRNA-15b-5p up-regulation on synapse-relevant genes *VAMP1* and *STXBP3A* was studied by qRT-PCR in the nucleus accumbens from control mice, CUMS-induced depression mice, and microRNA-15b-5p agomir-injection mice. microRNA-15b-5p agomir was injected into the nucleus accumbens. After various treatments, their mood was assessed by SPT, YMT, and FST. The tissues of the nucleus accumbens were harvested from these mice. The expression of *VAMP1* decreases from 100.16 ± 2% in control mice (*open symbols* in Fig. 13*A*; $n = 6$) to 41.60 ± 6.42% in the CUMS-induced depression mice (*red symbols*, $n = 6$) and to 26.64 ± 2.7% in microRNA-15b-5p agomir-injection mice (*yellow symbols*; $n = 6$, p values are less than 0.001 to 0.05, one-way ANOVA). The expression of *STXBP3A* decreases from 100.1 ± 1.62% in control mice (*open symbols* in Fig. 13*B*; $n = 6$) to 55.98 ± 5.24% in the CUMS-induced depression mice (*red symbols*, $n = 6$) and to 32.81 ± 4.82% in microRNA-15b-5p agomir-injection mice (*yellow symbols*; $n = 6$, p values are less than 0.001 to 0.05, one-way ANOVA). The CUMS-induced down-regulation of synapse-relevant genes *VAMP1* and *STXBP3A* in the nucleus accumbens is mimicked by microRNA-15b-5p derivatives.

The effect of microRNA-15b-5p up-regulation on synapse-relevant proteins VAMP1 and STXBP3A was examined by Western blotting in the nucleus accumbens from control mice, CUMS-induced depression mice, and microRNA-15b-5p agomir-injection mice. microRNA-15b-5p agomir was injected into the nucleus accumbens. The tissues of the nucleus accumbens were harvested from these mice. As showed in Fig. 13*C*, microRNA-15b-5p agomir appears to attenuate VAMP1 and STXBP3A in the nucleus accumbens similar to that by the CUMS. The expression of VAMP1 changes from 100.0 ± 8.22%

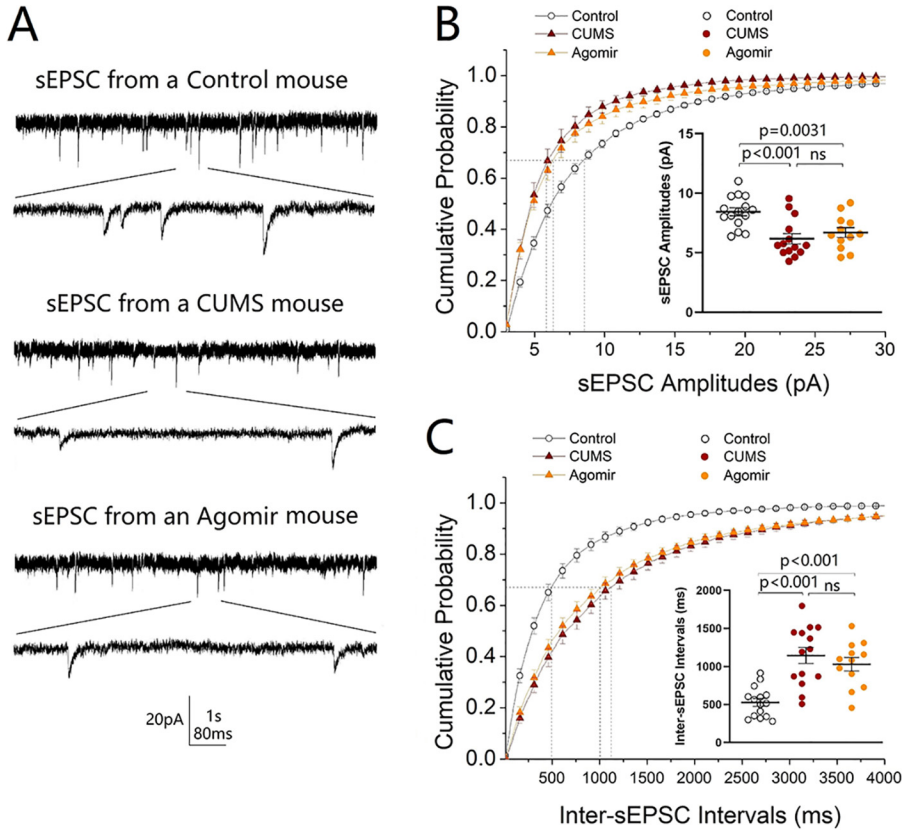

Figure 11. microRNA-15b-5p impairs synaptic transmission in GABAergic neurons of the NAc similarly to that induced by the CUMS. sEPSCs were recorded under voltage-clamp in the brain slices in the presence of 10 μM bicuculline. *A* shows sEPSCs from a control mouse (*top traces*), a CUMS-induced depression mouse (*middle traces*), and a microRNA-15b-5p agomir-injection mouse (*bottom traces*). Calibration symbols: *vertical symbols*, 20 pA; *horizontal,* 1 s (*top*) and 80 ms (*bottom*). *B* shows cumulative probability *versus* sEPSC amplitudes from control group (*open symbols*, $n = 15$ cells from five mice), CUMS-induced depression group (*red symbols*, $n = 14$ cells from five mice), and microRNA-15b-5p agomir-injection group (*yellow symbols*, $n = 12$ cells from five mice). *Dashed lines* indicate sEPSC amplitudes at CP67. The *inset* shows a comparison of sEPSC amplitudes at CP67 from control mice (*open symbols*), CUMS-induced depression-like mice (*red symbols*), and microRNA-15b-5p agomir-injection mice (*yellow symbols*). *C* shows cumulative probability *versus* inter-sEPSC intervals from control group (*open symbols*, $n = 15$ cells from five mice), CUMS-induced depression group (*red symbols*, $n = 14$ cells from five mice), and microRNA-15b-5p agomir-injection group (*yellow symbols*, $n = 12$ cells from five mice). *Dashed lines* indicate sEPSC intervals at CP67. The *inset* shows a comparison of sEPSC intervals at CP67 from control mice (*open symbols*), CUMS-induced depression mice (*red symbols*), and microRNA-15b-5p agomir-injection mice (*yellow symbols*). One-way ANOVA was used for statistical comparisons among control mice, CUMS-induced depression mice and microRNA-15b-5p agomir-injection mice. *ns*, no statistical significance.

in control mice (*open symbols* in Fig. 13*D*; $n = 6$) to 28.65 ± 5.73% in the CUMS-induced depression mice (*red symbols*, $n = 6$) and to 20.59 ± 5.2% in microRNA-15b-5p agomir-injection mice (*yellow symbols*; $n = 6$, $p < 0.01$, one-way ANOVA). The expression of STXBP3A changes from 100.0 ± 4.81% in control mice (*open symbols* in Fig. 13*E*; $n = 6$) to 52.72 ± 8.04% in the CUMS-induced depression mice (*red symbols*, $n = 6$) and to 37.19 ± 5.43% in microRNA-15b-5p agomir-injection mice (*yellow symbols*; $n = 6$, $p < 0.01$, one-way ANOVA). The CUMS-induced down-regulation of synapse proteins VAMP1 and STXBP3A in the nucleus accumbens is mimicked by microRNA-15b-5p derivatives. Thus, microRNA-15b-5p sufficiently suppresses the expression of genes and proteins (VAMP1 and STXBP3A) similar to that in the CUMS-induced depression.

Discussion

CUMS induces depression-like behavior, *e.g.* an increase of immobile time in the forced swim test as well as the decreases in sucrose preference and social interaction. This CUMS also weakens excitatory synaptic transmission and synapse innervation on GABAergic neurons in the nucleus accumbens from the medial prefrontal cortex as well as decreases the expression of genes and proteins relevant to the synapses, such as VAMP1 and STXBP3A. In other words, CUMS induces major depression by down-regulating the excitatory synapses, *e.g.* their presynaptic targets, on GABAergic neurons in the nucleus accumbens. In terms of the initiative factor from the CUMS to these molecular and cellular changes in the nucleus accumbens, our study shows that the up-regulation of microRNA-15b-5p induces depression-like behavior, and the down-regulation of microRNA-15b-5p significantly rescues CUMS-induced depression by influencing these cellular and molecular changes in relevance to GABAergic neurons in the nucleus accumbens. Therefore, the requirement and sufficiency of microRNA-15b for CUMS-induced depression and its relevant cellular and molecular changes indicate microRNA-15b-5p is essential for initiating CUMS-induced depression as well as anti-microRNA-15b-5p may be used to rescue major depression. The chain reaction that leads to CUMS-induced depression includes the CUMS, the elevated microRNA-15b-5p expression, the down-regulated VAMP1 and STXBP3A, as well as the

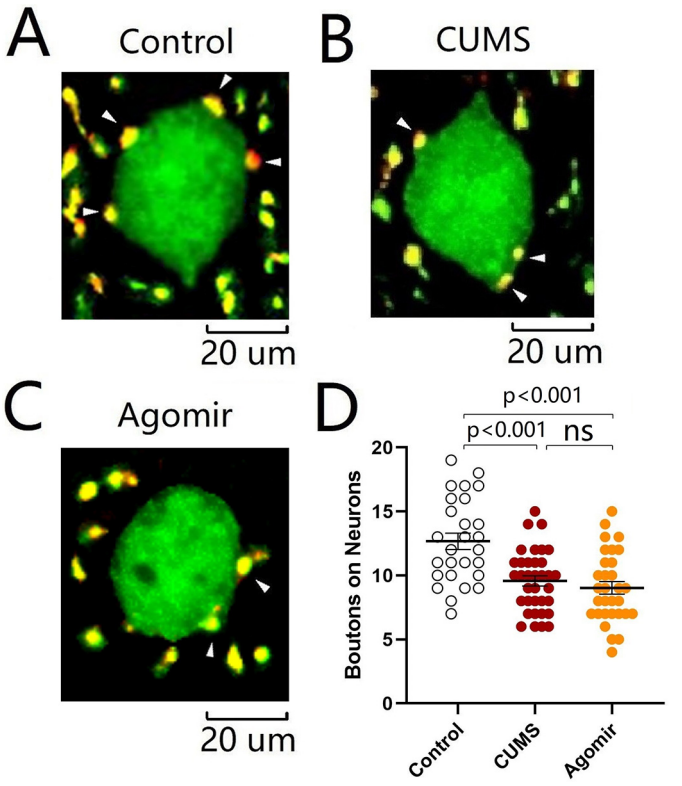

Figure 12. microRNA-15b-5p attenuates synapse innervations similarly to that induced by the CUMS. *A–C* show innervations (*yellow*) from mPFC to GABAergic neurons (*green*) of NAc in control mice (*A*), CUMS-induced depression mice (*B*), and microRNA-15b-5p agomir-injection mice (*C*). *D* shows the innervations from mPFC to GABAergic neurons of NAc in the control group (*open symbols*, $n = 27$ cells from five mice), CUMS-induced depression group (*red symbols*, $n = 35$ cells from five mice), and microRNA-15b-5p agomir-injection group (*yellow symbols*, $n = 31$ cells from five mice). One-way ANOVA was used for statistical comparisons among control mice, CUMS-induced depression mice, and microRNA-15b-5p agomir-injection mice. *ns*, no statistical significance.

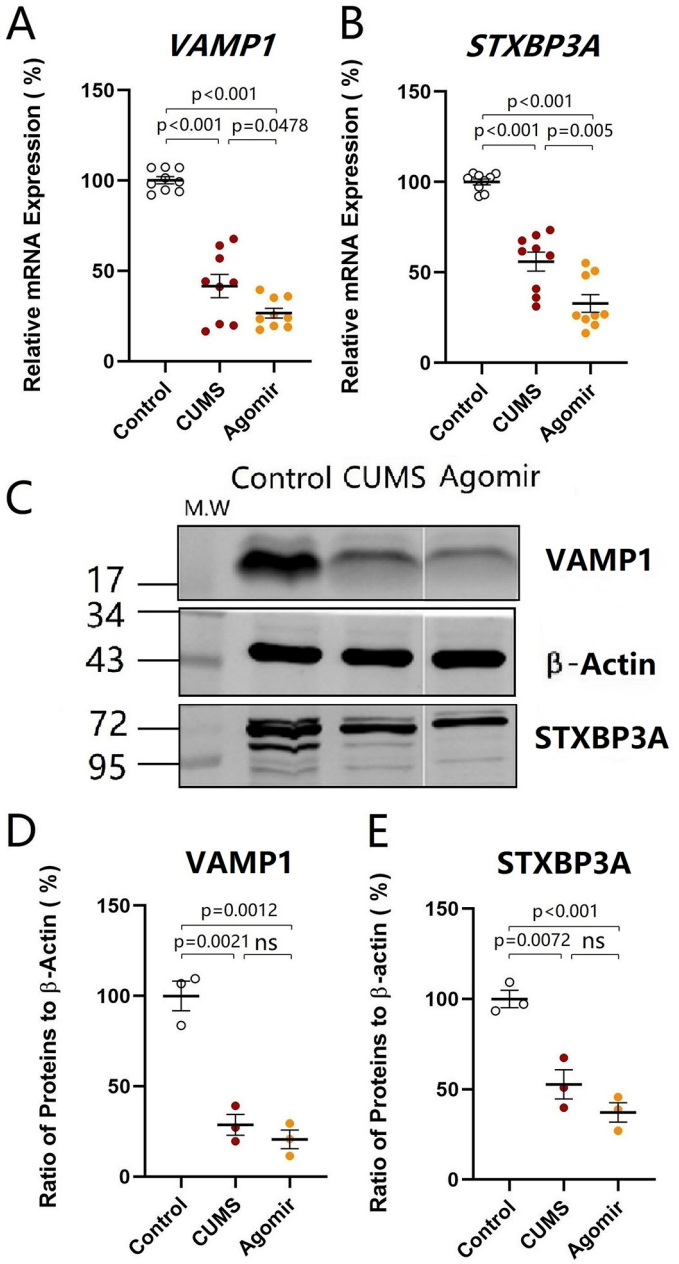

Figure 13. microRNA-15b-5p attenuates the expression of VAMP1 and STXBP3A similarly to that induced by the CUMS. The expression levels of mRNA *VAMP1* and *STXBP3A* were analyzed by quantitative RT-PCR. The expressions of proteins VAMP1 and STXBP3A were measured by Western blottings. *A* and *B* show the relative value of mRNA for *VAMP1* (*A*) and *STXBP3A* (*B*) in control mice (*open symbols*, $n = 6$), CUMS-induced depression mice (*red symbols*, $n = 6$), and microRNA-15b-5p agomir-injection mice (*yellow symbols*, $n = 6$), in which internal control is β-actin. *C* shows the expressions of VAMP1 and STXBP3A from control mice, CUMS-induced depression mice, and microRNA-15b-5p agomir-injection mice, in which internal control is β-actin. *D* and *E* illustrate the normalized ratios of VAMP1 (*D*) and STXBP3A (*E*) expression to β-actin from control mice (*open symbols*, $n = 6$), CUMS-induced depression mice (*red symbols*, $n = 6$), and microRNA-15b-5p agomir-injection mice (*yellow symbols*, $n = 6$). The relative ratios for control mice are normalized to be 1. One-way ANOVA was used for statistical comparisons among control mice, CUMS-induced depression mice, and microRNA-15b-5p agomir-injection mice. *Arrowheads* indicate synaptic contacts between presynaptic boutons and GABAergic cell bodies. *ns*, no statistical significance.

deteriorated presynaptic components of excitatory synapses on GABAergic neurons in the nucleus accumbens.

The deterioration of GABAergic neurons in the nucleus accumbens is the basis of depression-like behavior because the depression seems to be rescued by up-regulating their synapse innervations/functions as well as induced by their down-regulation. By manipulating microRNA-15b-5p–regulated genes and proteins in relevance to presynaptic targets, our data strengthen implications from those studies that GABAergic neurons in the nucleus accumbens are associated with stress-induced depression (51, 52, 54) and that mice in the resilience to chronic mild stress demonstrate the relatively normal function of GABAergic neurons in the nucleus accumbens (55). As the nucleus accumbens is presumably the important region of reward circuits (33–38), its dysfunction shifts the emotion balance toward the negative end, leading to anhedonia, interest loss, and low self-esteem.

In terms of the molecular mechanism underlying the CUMS-induced dysfunction of GABAergic neurons in the nucleus accumbens, our data indicate that the attenuated expression of VAMP1 and STXBP3A genes and proteins is associated with CUMS-induced depression (Fig. 4) and that this effect is based on the direct inhibitory interaction of microRNA-15b-5p to mRNAs relevant to encoding these two proteins (Fig. 5). Furthermore, microRNA-15b-5p antagomir significantly rescues CUMS-induced depression-like behavior as well as preserves

synapse function and innervations by up-regulating VAMP1 and STXBP3A (Figs. 6–9). microRNA-15b-5p derivative mimics CUMS-induced depression-like behavior and synapse deterioration by down-regulating VAMP1 and Stxbp3 (Figs. 10–13). Our studies suggest that microRNA-15b-5p by inhibiting vesicle-release proteins VAMP1 and STXBP3A may impair excitatory synapses on GABAergic neurons in the nucleus accumbens and induces depression-like behavior. Other molecular and cellular processes regulated by microRNA-15b in the nucleus accumbens may be involved in major depression, which remains to be tested.

It is noteworthy that other molecules in the nucleus accumbens have been found to be related to depression-like behavior. For instance, Tet1 in the nucleus accumbens opposes depression-like behavior (49). In the nucleus accumbens, the down-regulations of serotonergic and dopaminergic synapses as well as of the MAPK and calcium-signaling pathways are associated with CUMS-induced depression. The up-regulations of PI3K–Akt and cAMP signaling pathways and amino acid metabolism are associated with CUMS-induced depression (25). As all these molecules in the nucleus accumbens may be associated with major depression, microRNA-15b-5p partially preserves CUMS-induced depression by up-regulating the expression of synaptic proteins and the excitatory driving force on GABAergic neurons in the nucleus accumbens (Figs. 10–13). Moreover, our study by up-regulating and down-regulating microRNA-15b-5p to conclude its essential role in major depression is compelling, compared with those previous studies that show the associated changes between molecules and behavior only.

In addition, a previous study (56) indicates the involvement of amygdala microRNA-15a in chronic stress. microRNA-19b associates with Ago2 in the amygdala after chronic stress and regulates the adrenergic β1-receptor (63). microRNA-15b-5p is up-regulated in the cerebral cortices of depression-like mice by acting to synapse-relevant proteins (22). How microRNA-15a, microRNA-19b, and microRNA-15b-5p in the amygdala and nucleus accumbens coordinately lead to major depression remains to be investigated. Moreover, numerous microRNAs and mRNAs in the nucleus accumbens, amygdala, and ventral tegmental area are associated with depression-like behavior (24, 25, 27). How these microRNAs and mRNAs relevant to synapses and neural signaling pathways among these brain areas coordinately induce major depression remains to be investigated. As microRNA-15b-5p significantly leads to depression-like behavior, it should be one of critical molecules for the incidence of major depression.

The nucleus accumbens is considered as an important region of brain reward circuits (33–38), especially an important structure to regulate emotion reaction and cognitive events (36, 39–41). The nucleus accumbens possesses the mutual synapse innervations with many brain regions, such as the ventral tegmental area, the prefrontal cortex, and the amygdala. Its physiological roles presumably involve various psychological processes, such as emotion, motivation, cognition, and action, as well as to encode the reward feeling from the food taking and drug addiction (13, 36, 43, 64–66). As the nucleus accumbens receives synapse innervations from the ventral tegmental area and the prefrontal cortex for the reward-driven events, the down-regulation of presynaptic proteins VAMP1 and Stxbp3 by anti-microRNA-15b may affect all of these presynaptic terminals onto nucleus accumbens neurons. Their dysfunction by activity silence may lead to anhedonia, interest loss, and low motivation in major depression (52). Together, these data suggest that the induction of major depression may be due to a lack of reward that leads to the poor activation of brain reward circuits (55); this is being tested.

Although chronic stress is a main etiology of major depressive disorders (1–5, 67–69), most of the individuals after experiencing chronic stress do not suffer from major depression, *i.e.* a resilience to the chronic stress (14). It has been found that the functions of GABAergic neurons in the nucleus accumbens are close to normal in CUMS-resilience mice (55), indicating that there may be endogenous anti-depression mechanisms in the nucleus accumbens for the animals to be resilient to chronic stress. In the nucleus accumbens, the down-regulations of the chemokine-signaling pathway, synaptic vesicle cycle, and nicotine addiction and the up-regulations of the calcium-signaling pathway and tyrosine metabolism are associated with CUMS resilience (25, 70). An induction of ΔFosB in the nucleus accumbens in response to chronic social defeat stress was both necessary and sufficient for resilience (71). Taking these previous studies together with our results that microRNA-15b-5p down-regulation of and its preservation to the low expression of VAMP1 and STXBP3A appear to significantly reduce the incidence of CUMS-induced depression, we assume that an endogenous mechanism for animals to be resistant to chronic stress is based on a molecular network. The elucidation of the endogenous mechanism for the resilience to the chronic stress should shed light on developing therapeutic strategies for major depression. The ventral tegmental area, nucleus accumbens, amygdala, and medial prefrontal cortex are accounted into the brain reward circuit (72–74). These structures contain GABAergic neurons, especially the core area of the amygdala, and the nucleus accumbens mainly include the cluster of GABAergic neurons. The impairment of GABAergic neurons in the limbic system is associated with major depression (55, 62, 75–89). Whether the intact function of the GABAergic neurons in these regions beyond the nucleus accumbens is also associated with resilience to chronic stress remains to be examined in order to get a general view that the functional state of GABAergic neurons in the brain is correlated with the resilience *versus* susceptibility to chronic stress for major depression.

Experimental procedures

Subjects were male C57 GAD67–GFP mice (3 weeks of age) housed in cages (32 × 16 × 16 cm, length × width × height) with free access to food and water and maintained in a well-conditioned room with controlled temperature (22 ± 2 °C), humidity (55 ± 5%), and a light/dark cycle of 12 h (illumination at 7:00–19:00). Experimental procedures were accredited by Institutional Animal Care and Use Committee (B10831). Experiments were conducted in compliance with the rules and guidelines of the Administration Office of Laboratory Animals, Beijing, China.

Mouse model of major depression induced by CUMS

Strain C57 GAD67–GFP mice (90) were used for the study of the cell-specific mechanism of NAc-related depression because the GABAergic neurons of this strain were genetically labeled by green fluorescent protein (GFP). Postnatal 21-day C57 male mice were used for our experiments that were based on the studies that young individuals were more susceptible to chronic stress (27, 55, 88). After a 1-week accommodation, their performance on locomotion, sucrose preference, and Y-maze tests were recorded as the self-control data. Mice at postnatal day 28 that had consistent behavioral values (within mean ± 2SD of three tests) were randomly divided into the control, CUMS, antagomir injection plus CUMS, and agomir injection groups. The CUMS treatments were absent for the control and agomir injection mice. C57 male mice were used on the basis of previous research (91–93).

The CUMS was used to induce major depression in mice (22, 62, 88). Mice living in an inescapable stressful environment constantly experienced defeated outcomes. Some mice showed depression-like symptoms like anhedonia and low self-esteem after exposure to CUMS, which induces repetitive negative memory that drives the mice to feel cognitive disability and emotional frustration (13, 24, 25, 27, 66, 94, 95). The paradigms of 3-week CUMS consisted of social isolation, empty cage, tilted cage, wet sawdust cage, white noise, restraint, circadian disturbance, and strobe light (22, 55, 62, 88). Except for the social isolation, other stressors were randomly given to mice individually or in combination everyday (please refer to Table 1 in Ref. 88 for more detail).

The CUMS-induced depression-like symptoms such as anhedonia and low self-esteem were examined at days 36–39. Anhedonia was measured by SPT. Loss of interest for social interaction was evaluated by YMT. The state of self-esteem was assessed by FST (7, 88, 96, 97). During the 4-h SPT, the ingestion of 1% sucrose water and normal water was measured. Sucrose preference values were calculated as the percentage of the ingested sucrose water to total ingested water. The YMT was performed by recording the mouse staying time in a special arm and other two arms. At the terminus of the special arm (defined as M-arm), a female mouse caged in the glass box (punched with many round holes) was placed to attract the subject mouse for social interaction. After a 3-min recording, M-arm stay time was presented by the percentage of stay time in M-arm to three arms. The FST was conducted by recording the length of immobility while mice floated in a water cylinder (diameter = 10 cm, depth = 19 cm, 25 °C). The SPT and YMT were conducted before and after the CUMS, while the FST was done once. Before the SPT, mice were deprived of water and food for 3 h to invoke their eagerness to drink water. After each YMT, three arms were cleaned by 70% ethanol and then with water to erase the residual odor. Before the behavior tests, mice were absent from stressors and were allowed to accommodate themselves in the testing environment. All behavior tests were conducted in a quiet room with controlled temperature (25 °C) and humans (55 ± 5%) (22, 62, 88).

After comparison with the behavioral performance of them (day 0) and the control mice, depression-like behavior was verified by the reduction in sucrose preference, M-arm stay time, and the increase length of immobility. The behavior performance of each mouse would be regarded as a significant change if the sucrose preference and M-arm stay time were reduced above 20% when compared with its self-control, and the immobile time was increased above 15% when compared with the control group. These standards were set up on the basis of the averaged behavioral performance in mice during our previous tests (24, 25, 27, 55, 62, 88).

Microinjection of microRNA-15b-5p antagomir or agomir into the nucleus accumbens

miRNA antagomir was the chemically-modified cholesterol-conjugated single-stranded RNA analogues complementary to specific miRNAs. In a previous study (98), the antagomir designed for inhibiting miRNA was based on the rule of their base complementary, and their binding has been found to specifically inhibit miRNA expression. This approach has been proved to be well-matured. In our study, microRNA-15b-5p antagomir was an RNA analogue complementary to microRNA-15b-5p. microRNA-15b-5p agomir was a derivative of chemically-synthesized microRNA-15b-5p. Antagomir or agomir control is miRNA with its sequence based on *Caenorhabditis elegans*. As it has no identifiable effects on mammals, it has served as the negative control of miRNA antagomir or agomir. microRNA-15b-5p antagomir, agomir, and their negative control were purchased from Ruibo Biological Technology (Guangzhou, China). Mice were anesthetized by intraperitoneal injection of 4% chloral hydrate (0.1 ml/10 g), and their heads were fixed on the stereotaxic device. 1 nM antagomir, agomir, or their negative control dissolved in 1 μl of ACSF was slowly injected (30–40 min) into NAc (1.2 mm before the bregma, 1.0 mm lateral to the midline, and 3.5 mm in the depth) three times every 3 days. The glass pipettes were use for the microinjections by adding air pressure from the microsyringe (RWD Life Science, Shenzhen, China).

Brain slices and neurons

To obtain more health neurons for whole-cell recordings, we prepared the brain slices, including NAc, by using the following protocols. Mice were anesthetized by inhaling isoflurane, and their left ventricles were infused by the ACSF (4 °C, oxygenated by 95% O_2 and 5% CO_2) until their limbs turned pale. The concentrations (mM) of ACSF were 124 NaCl, 3 KCl, 26 $NaHCO_3$, 1.2 NaH_2PO_4, 4 $MgSO_4$, 0.5 $CaCl_2$, 10 dextrose, and 220 sucrose at pH 7.35. Mice were quickly decapitated by guillotine, and the heads were submerged into oxygenated ACSF (4 °C) to isolate the brain tissue. Brain tissues were sliced (300 μm) in the oxygenated ACSF (4 °C) in a coronal direction by the Vibratome. The brain slices were transferred to another oxygenated ACSF (124 mM NaCl, 3 mM KCl, 1.2 mM NaH_2PO_4, 26 mM $NaHCO_3$, 2 mM $CaCl_2$, 2 mM $MgSO_4$, 10 mM dextrose, and 5 mM HEPES, at pH 7.35) at 25 °C and incubated for 2 h. During the whole-cell recordings, the brain slice was submerged in a chamber (Warner RC-26G) infused with oxygenated ACSF at 31 °C (99–101). The chemical reagents were from Sigma.

GFP-labeled GABAergic neurons in the NAc for whole-cell recordings were confirmed under differential interference

contrast–fluorescent microscope (Nikon FN-E600, Tokyo, Japan). The excitation wavelength of GFP is 488 nm. GABAergic neurons were featured by expressing fast spikes with less adaptive frequency and amplitude, which is typical for the interneurons (102–106).

Whole-cell recording for synaptic activities

The synaptic activity was recorded by MultiClamp-700B amplifier under the voltage-clamp, and intrinsic property was analyzed by current-clamp. Electrical signals were collected and analyzed by pClamp-10 (Axon Instrument Inc.). The output frequency of amplifier bandwidth was maintained at 3 kHz. The micropipette solution used for recording synaptic transmission included (mM) 150 K-gluconate, 5 NaCl, 5 HEPES, 0.4 EGTA, 4 Mg-ATP, 0.5 Tris-GTP, and 5 phosphocreatine (pH 7.35) (107–109). The micropipettes were newly-made, and internal solution was freshly prepared and filtered (0.1 μm). The osmolarity was 295–305 mosmol and the resistance of micropipette tip was 5–6 megohms.

The electrophysiological function of GABAergic neurons was evaluated via their excitatory synapse activity (110, 111). To isolate sEPSCs from synaptic currents, slices were infused by 10 μM bicuculline to eliminate $GABA_A$R-mediated inhibitory synaptic currents. To confirm that sEPSCs are mediated by ionotropic glutamate receptors (112, 113), 40 μM D-amino-5-phosphonovanolenic acid (DAP5) and 10 μM 6-cyano-7-nitroquinoxaline-2,3-(1*H*,4*H*)-dione that blocked sEPSCs were blended in the ACSF before the end of recording.

The whole-cell recording data were analyzed only if the recorded neurons had the resting membrane potentials below −60 mV and action potential amplitudes above 90 mV and also included less than 5% fluctuation of spike amplitudes, resting membrane potential, and input resistances during each recording. To monitor the series and input resistances of recorded neurons, hyperpolarization pulses (5 mV/50 ms) were injected. The resistances were calculated as pulses voltages divided by instantaneous and steady-state currents.

Morphological imaging of structural connections

Structural connections from medial prefrontal cortex (mPFC) to NAc were traced by injecting anterograde tracer pAAV–SynaptoTag–mCherry–GFP (by courtesy of Dr. Thomas Südhof) into the mPFC and detecting its projection to the NAc (90). In terms of the working principle of this AAV, synapsin-I promoter initiated the expression of enhanced GFP–synaptobrevin-2 in presynaptic boutons and the expression of mCherry in entire neurons, especially axons (114). According to the map of mouse brain (115), glass micropipettes were positioned in mPFC (1.8 mm prior to the bregma, 0.4 mm lateral to midline, and 1.5 mm in depth) during the pAAV injections. The excitation and emission wavelengths of mCherry were 565 and 610 nm, which were used to identify axon projection from mPFC to the NAc. Four weeks after the injection, the axon projection from mPFC to the NAc neurons were visualized by the confocal imaging.

After a 1-week recovery from stereotaxic surgery, mice were exposed to the CUMS or control condition. Once all behavioral tests were done, the mice were anesthetized by intraperitoneal injection of urethane (1.5 g/kg), and their left ventricles then were slowly perfused with 4% paraformaldehyde in 0.1 M phosphate-buffered solution (PBS) until their limbs turned stiff and pale. Brains were extracted and soaked in 4% paraformaldehyde PBS for 24-h fixation. Brain tissues, including NAc, were sliced (80 μm) in the coronal direction by the Vibratome. Slices were gently washed in PBS for 10 min, air-dried, and cover-slipped.

Morphological structure of mCherry-labeled boutons and GFP-labeled GABAergic neurons in the NAc were captured under the confocal microscope (Nikon A1R plus, Tokyo, Japan). Excitation wavelengths of mCherry and GFP were 565 and 488 nm. The optical grating for GFP and RFP were 500–550 and 570–620 nm. The merged images illustrated the synapse contacts. The resolution of confocal scanning was maintained at 0.05 μm/pixel (116–118).

To improve the clarity of boutons and neurons, brain slices were soaked in Sca*l*eA2 solution for 24 h (119, 120). The morphology and density of synapse contacts were visualized and counted in the shell and core of the NAc by using ImageJ (version 1.8.0; National Institutes of Health) and Imaris (version 9.3; Bitplane, UK). Structural contacts between mCherry-labeled boutons and GFP-labeled GABAergic neurons identified in the merged images under confocal microcopy were presumed to be synapses. We counted the number of synaptic contacts per neuron in the NAc.

Quantitative RT-PCR to validate the regulation of microRNA-15b-5p to mRNAs

SYBR Green-based quantitative PCRs were used for mRNA expression assay of genes *VAMP1* and *STXBP3A*. Total RNAs were extracted from NAc tissues by using the TRIzol kit. cDNAs for mRNA expression analysis were reverse-transcripted by using the PrimeScript RT reagent kit (TaKaRa, RR037A, Kusatsu/Shiga, Japan). Reverse transcription of mRNA was performed in 20-μl reactions composed of 1 μl of template cDNA and 0.5 μl of forward and 0.5 μl of reverse primers (10 nmol/liter), 10 μl of 2× qPCR Mastermix (SYBR Green), and 8 μl of double distilled H_2O. Real-time qPCR was performed on the Bio-Rad CFX96 Touch. The reaction started with initial denaturation for 2 min at 95 °C, followed by 40 cycles of denaturation for 15 s at 95 °C, annealing, and extension for 30 s at 60 °C, and ended by obtaining the melt curve from 65 to 95 °C (increments of 0.5 °C per 5 s). The expression of miR-15b-5p–targeted mRNAs was normalized to the internal control β-actin. The results were calculated with the $2^{-\Delta\Delta Ct}$ method (53). All real-time qPCRs of each treatment were run in triplicate.

Dual-luciferase reporter assay

The sequence carrying the targeted sites of miR-15b-5p targeting genes *VAMP1* and *STXBP3A* were amplified, cut by NotI and XhoI, and restructured into the luciferase reporter vector psiCHECK2 (22, 62). The miR-15b-5p targeting sites were site-directed mutated by QuikChange Lighting site-directed mutagenesis kit (Stratagene, La Jolla, CA) following the instructions of the manufacturer. Luciferase reporter detection assays were conducted following the previous description (62). HEK293T cells were planted on 24-well plates (5×10^4 cells per

well) and cultured in Dulbecco's modified Eagle's medium with 10% fetal bovine serum added. After 24 h, HEK293T cells were transfected by 50 ng of WT psiCHECK2 or mutant luciferase reporter plasmids and 50 nM miRNAs mimic or negative control by using Lipofectamine® 2000 transfection reagent (Invitrogen). After 48 h, the activities of *Renilla* and firefly luciferase were measured by Dual-Glo® luciferase assay system (Promega) under the instructions of the manufacturer. Each treatment was run in triplicate in three independent experiments.

Western blottings to quantify protein

The NAc tissues extracted from mouse brains were gently washed 20 s in PBS (4 °C) and quickly transferred to 1 ml of RIPA Lysate buffer (4 °C) with 1 mM phenylmethylsulfonyl fluoride (Beyotime Biotechnology, China) added for complete homogenization. Homogenized tissues were placed into a fresh tube, held on ice for 30 min, and centrifuged at 12,000 × *g*/min for 15 min at 4 °C. The supernatant was collected into a new tube. Total protein concentration of supernatant was estimated by using BCA protein assay under the instructions of the manufacturer (Beyotime Biotechnology, Shanghai, China). We prepared the 5 and 12% SDS-polyacrylamide gel for electrophoresis to separate VAMP1 and STXBP3A from each sample. Twenty micrograms of total proteins per sample an the molecular weight markers were loaded into the wells of the SDS-polyacrylamide gel, and electrophoresis was run for 1 h. We electrically transferred the protein from the gel to the nitrocellulose membranes (0.2 μm). The membranes were blocked by 5% nonfat milk solution (dissolved in 1× TBS with addition of 0.1% Tween 20) at 25 °C for 60 min. We then incubated the membrane with primary antibodies (1:1000 in dilution) of VAMP1 (13151S, Cell Signaling Technology), STXBP3A (13764-1-AP, Proteintech, Wuhan, China), and β-actin (AC026, AB Clonal Technology, Wuhan, China) overnight. After incubation with primary antibody, the membranes were washed by PBS for 10 min (three times). We incubated the membrane with secondary antibodies DyLight 680 (5470S, Thermo Fisher Scientific) for 1 h. Bands of VAMP1, STXBP3A, and β-actin were visualized by using IR imaging system Odyssey® CLx (LI-COR, Lincoln, NE). The fluorescence of each band was determined after the adjustment of background for relative quantitative analysis. The fluorescence of each band was normalized to the internal control β-actin and analyzed using ImageJ software (version 1.47; National Institutes of Health).

Statistical analyses

The data of behavioral tests, electrophysiological recordings, and protein chemistry are presented as the means ± S.E. Comparisons of behavioral data in each of the mice before and after CUMS was made by paired *t* test. Comparisons of neuronal function, structural connection, and molecular expression among control, CUMS-induced depression mice, microRNA-15b-5p antagomir plus CUMS, and microRNA-15b-5p agomir were made by one-way ANOVA. Animal experiments and data analysis were assigned to different investigators in a blinded way to ensure the unawareness of information about the group and manipulation. Statistical data were analyzed by using Origin (version 8; Northampton, MA) and GraphPad Prism (version 7.00; La Jolla, CA).

Data availability

All data are contained within the manuscript.

Author contributions—L. G., Z. Z., and G. W. software; L. G., Z. Z., G. W., and M. S. formal analysis; L. G., Z. Z., G. W., and M. S. investigation; L. G., Z. Z., G. W., and M. S. visualization; L. G., Z. Z., G. W., and M. S. methodology; J.-H. W. writing-review and editing; S. C. and Z. S. data curation; J.-H. W. supervision; J.-H. W. resources; J.-H. W. conceptualization; J.-H. W. writing-original draft.

Acknowledgment—We thank Dr. Thomas Südhof for pAAV–SynaptoTag–mCherry–GFP.

References

1. Hamilton, J. P., Chen, M. C., and Gotlib, I. H. (2013) Neural systems approaches to understanding major depressive disorder: an intrinsic functional organization perspective. *Neurobiol. Dis.* **52,** 4–11 CrossRef Medline
2. Jabbi, M., Korf, J., Ormel, J., Kema, I. P., and den Boer, J. A. (2008) Investigating the molecular basis of major depressive disorder etiology: a functional convergent genetic approach. *Ann. N.Y. Acad. Sci.* **1148,** 42–56 CrossRef Medline
3. Keers, R., and Uher, R. (2012) Gene-environment interaction in major depression and antidepressant treatment response. *Curr. Psychiatry Rep.* **14,** 129–137 CrossRef Medline
4. Lohoff, F. W. (2010) Overview of the genetics of major depressive disorder. *Curr. Psychiatry Rep.* **12,** 539–546 CrossRef Medline
5. Moylan, S., Maes, M., Wray, N. R., and Berk, M. (2013) The neuroprogressive nature of major depressive disorder: pathways to disease evolution and resistance, and therapeutic implications. *Mol. Psychiatry* **18,** 595–606 CrossRef Medline
6. Banasr, M., Dwyer, J. M., and Duman, R. S. (2011) Cell atrophy and loss in depression: reversal by antidepressant treatment. *Curr. Opin. Cell Biol.* **23,** 730–737 CrossRef Medline
7. Duman, C. H. (2010) Models of depression. *Vitam. Horm.* **82,** 1–21 CrossRef Medline
8. Bennett, P., Wilkinson, C., Turner, J., Brain, K., Edwards, R. T., Griffith, G., France, B., and Gray, J. (2008) Psychological factors associated with emotional responses to receiving genetic risk information. *J. Genet. Couns.* **17,** 234–241 CrossRef
9. Elizalde, N., Gil-Bea, F. J., Ramírez, M. J., Aisa, B., Lasheras, B., Del Rio, J., and Tordera, R. M. (2008) Long-lasting behavioral effects and recognition memory deficit induced by chronic mild stress in mice: effect of antidepressant treatment. *Psychopharmacology* **199,** 1–14 CrossRef Medline
10. Lin, L. C., and Sibille, E. (2013) Reduced brain somatostatin in mood disorders: a common pathophysiological substrate and drug target? *Front. Pharmacol.* **4,** 110 CrossRef Medline
11. Pittenger, C., and Duman, R. S. (2008) Stress, depression, and neuroplasticity: a convergence of mechanisms. *Neuropsychopharmacology* **33,** 88–109 CrossRef Medline
12. Sandi, C., and Haller, J. (2015) Stress and the social brain: behavioural effects and neurobiological mechanisms. *Nat. Rev. Neurosci.* **16,** 290–304 CrossRef Medline
13. Wang, J. H. (2019) *Associative Memory Cells: Basic Units of Memory Trace* (Wang, J.-H., ed), 1st Ed., pp. 1–275, Springer Nature, Singapore
14. Southwick, S. M., and Charney, D. S. (2012) The science of resilience: implications for the prevention and treatment of depression. *Science* **338,** 79–82 CrossRef Medline
15. Bai, M., Zhu, X. Z., Zhang, Y., Zhang, S., Zhang, L., Xue, L., Zhong, M., and Zhang, X. (2014) Anhedonia was associated with the dysregulation of hippocampal HTR4 and microRNA Let-7a in rats. *Physiol. Behav.* **129,** 135–141 CrossRef Medline
16. Bergström, A., Jayatissa, M. N., Thykjaer, T., and Wiborg, O. (2007) Molecular pathways associated with stress resilience and drug resistance

in the chronic mild stress rat model of depression: a gene expression study. *J. Mol. Neurosci.* **33,** 201–215 CrossRef Medline
17. Dias, C., Feng, J., Sun, H., Shao, N. Y., Mazei-Robison, M. S., Damez-Werno, D., Scobie, K., Bagot, R., LaBonté, B., Ribeiro, E., Liu, X., Kennedy, P., Vialou, V., Ferguson, D., Peña, C., *et al.* (2014) β-Catenin mediates stress resilience through Dicer1/microRNA regulation. *Nature* **516,** 51–55 CrossRef Medline
18. Higuchi, F., Uchida, S., Yamagata, H., Abe-Higuchi, N., Hobara, T., Hara, K., Kobayashi, A., Shintaku, T., Itoh, Y., Suzuki, T., and Watanabe, Y. (2016) Hippocampal microRNA-124 enhances chronic stress resilience in mice. *J. Neurosci.* **36,** 7253–7267 CrossRef Medline
19. Li, J. Z., Bunney, B. G., Meng, F., Hagenauer, M. H., Walsh, D. M., Vawter, M. P., Evans, S. J., Choudary, P. V., Cartagena, P., Barchas, J. D., Schatzberg, A. F., Jones, E. G., Myers, R. M., Watson, S. J., Jr., Akil, H., and Bunney, W. E. (2013) Circadian patterns of gene expression in the human brain and disruption in major depressive disorder. *Proc. Natl. Acad. Sci. U.S.A.* **110,** 9950–9955 CrossRef Medline
20. Liu, B. B., Luo, L., Liu, X. L., Geng, D., Liu, Q., and Yi, L. T. (2015) 7-Chlorokynurenic acid (7-CTKA) produces rapid antidepressant-like effects: through regulating hippocampal microRNA expressions involved in TrkB-ERK/Akt signaling pathways in mice exposed to chronic unpredictable mild stress. *Psychopharmacology* **232,** 541–550 CrossRef Medline
21. Moreau, M. P., Bruse, S. E., David-Rus, R., Buyske, S., and Brzustowicz, L. M. (2011) Altered microRNA expression profiles in postmortem brain samples from individuals with schizophrenia and bipolar disorder. *Biol. Psychiatry* **69,** 188–193 CrossRef Medline
22. Ma, K., Guo, L., Xu, A., Cui, S., and Wang, J. H. (2016) Molecular mechanism for stress-induced depression assessed by sequencing miRNA and mRNA in medial prefrontal cortex. *PLoS ONE* **11,** e0159093 CrossRef Medline
23. Rajkowska, G., Mahajan, G., Maciag, D., Sathyanesan, M., Iyo, A. H., Moulana, M., Kyle, P. B., Woolverton, W. L., Miguel-Hidalgo, J. J., Stockmeier, C. A., and Newton, S. S. (2015) Oligodendrocyte morphometry and expression of myelin-related mRNA in ventral prefrontal white matter in major depressive disorder. *J. Psychiatr. Res.* **65,** 53–62 CrossRef Medline
24. Shen, M., Song, Z., and Wang, J. H. (2019) microRNA and mRNA profiles in the amygdala are associated with stress-induced depression and resilience in juvenile mice. *Psychopharmacology* **236,** 2119–2142 CrossRef Medline
25. Si, Y., Song, Z., Sun, X., and Wang, J. H. (2018) microRNA and mRNA profiles in nucleus accumbens underlying depression versus resilience in response to chronic stress. *Am. J. Med. Genet. B Neuropsychiatr. Genet.* **177,** 563–579 CrossRef Medline
26. Smalheiser, N. R., Lugli, G., Rizavi, H. S., Zhang, H., Torvik, V. I., Pandey, G. N., Davis, J. M., and Dwivedi, Y. (2011) MicroRNA expression in rat brain exposed to repeated inescapable shock: differential alterations in learned helplessness vs. nonlearned helplessness. *Int. J. Neuropsychopharmacol.* **14,** 1315–1325 CrossRef Medline
27. Sun, X., Song, Z., Si, Y., and Wang, J. H. (2018) microRNA and mRNA profiles in ventral tegmental area relevant to stress-induced depression and resilience. *Prog. Neuropsychopharmacol. Biol. Psychiatry* **86,** 150–165 CrossRef Medline
28. Smalheiser, N. R., Lugli, G., Rizavi, H. S., Torvik, V. I., Turecki, G., and Dwivedi, Y. (2012) MicroRNA expression is down-regulated and reorganized in prefrontal cortex of depressed suicide subjects. *PLoS ONE* **7,** e33201 CrossRef Medline
29. Afonso-Grunz, F., and Müller, S. (2015) Principles of miRNA–mRNA interactions: beyond sequence complementarity. *Cell. Mol. Life Sci.* **72,** 3127–3141 CrossRef Medline
30. Beilharz, T. H., Humphreys, D. T., and Preiss, T. (2010) miRNA effects on mRNA closed-loop formation during translation initiation. *Prog. Mol. Subcell. Biol.* **50,** 99–112 CrossRef Medline
31. Dalmay, T. (2013) Mechanism of miRNA-mediated repression of mRNA translation. *Essays Biochem.* **54,** 29–38 CrossRef Medline
32. Valinezhad Orang, A., Safaralizadeh, R., and Kazemzadeh-Bavili, M. (2014) Mechanisms of miRNA-mediated gene regulation from common downregulation to mRNA-specific upregulation. *Int. J. Genomics* **2014,** 970607 CrossRef Medline
33. Basar, K., Sesia, T., Groenewegen, H., Steinbusch, H. W., Visser-Vandewalle, V., and Temel, Y. (2010) Nucleus accumbens and impulsivity. *Prog. Neurobiol.* **92,** 533–557 CrossRef Medline
34. Day, J. J., and Carelli, R. M. (2007) The nucleus accumbens and Pavlovian reward learning. *Neuroscientist* **13,** 148–159 CrossRef Medline
35. Carlezon, W. A., Jr., and Thomas, M. J. (2009) Biological substrates of reward and aversion: a nucleus accumbens activity hypothesis. *Neuropharmacology* **56,** Suppl. 1, 122–132 CrossRef Medline
36. Floresco, S. B. (2015) The nucleus accumbens: an interface between cognition, emotion, and action. *Annu. Rev. Psychol.* **66,** 25–52 CrossRef Medline
37. Ikemoto, S. (2007) Dopamine reward circuitry: two projection systems from the ventral midbrain to the nucleus accumbens-olfactory tubercle complex. *Brain Res. Rev.* **56,** 27–78 CrossRef Medline
38. Salamone, J. D., Correa, M., Mingote, S. M., and Weber, S. M. (2005) Beyond the reward hypothesis: alternative functions of nucleus accumbens dopamine. *Curr. Opin. Pharmacol.* **5,** 34–41 CrossRef Medline
39. Haruno, M., Kimura, M., and Frith, C. D. (2014) Activity in the nucleus accumbens and amygdala underlies individual differences in prosocial and individualistic economic choices. *J. Cogn. Neurosci.* **26,** 1861–1870 CrossRef Medline
40. Monk, C. S., Klein, R. G., Telzer, E. H., Schroth, E. A., Mannuzza, S., Moulton, J. L., 3rd., Guardino, M., Masten, C. L., McClure-Tone, E. B., Fromm, S., Blair, R. J., Pine, D. S., and Ernst, M. (2008) Amygdala and nucleus accumbens activation to emotional facial expressions in children and adolescents at risk for major depression. *Am. J. Psychiatry* **165,** 90–98 CrossRef Medline
41. Tzschentke, T. M., and Schmidt, W. J. (2000) Functional relationship among medial prefrontal cortex, nucleus accumbens, and ventral tegmental area in locomotion and reward. *Crit. Rev. Neurobiol.* **14,** 131–142 Medline
42. Fadok, J. P., Darvas, M., Dickerson, T. M., and Palmiter, R. D. (2010) Long-term memory for Pavlovian fear conditioning requires dopamine in the nucleus accumbens and basolateral amygdala. *PLoS One* **5,** e12751 CrossRef Medline
43. Hikida, T., Morita, M., and Macpherson, T. (2016) Neural mechanisms of the nucleus accumbens circuit in reward and aversive learning. *Neurosci. Res.* **108,** 1–5 CrossRef Medline
44. Kochenborger, L., Zanatta, D., Berretta, L. M., Lopes, A. P., Wunderlich, B. L., Januário, A. C., Neto, J. M., Terenzi, M. G., Paschoalini, M. A., and Faria, M. S. (2012) Modulation of fear/anxiety responses, but not food intake, following α-adrenoceptor agonist microinjections in the nucleus accumbens shell of free-feeding rats. *Neuropharmacology* **62,** 427–435 CrossRef Medline
45. Russo, S. J., Dietz, D. M., Dumitriu, D., Morrison, J. H., Malenka, R. C., and Nestler, E. J. (2010) The addicted synapse: mechanisms of synaptic and structural plasticity in nucleus accumbens. *Trends Neurosci.* **33,** 267–276 CrossRef Medline
46. Thomas, K. L., Hall, J., and Everitt, B. J. (2002) Cellular imaging with zif268 expression in the rat nucleus accumbens and frontal cortex further dissociates the neural pathways activated following the retrieval of contextual and cued fear memory. *Eur. J. Neurosci.* **16,** 1789–1796 CrossRef Medline
47. Yang, F. C., and Liang, K. C. (2014) Interactions of the dorsal hippocampus, medial prefrontal cortex and nucleus accumbens in formation of fear memory: difference in inhibitory avoidance learning and contextual fear conditioning. *Neurobiol. Learn. Mem.* **112,** 186–194 CrossRef Medline
48. Bosch-Bouju, C., Larrieu, T., Linders, L., Manzoni, O. J., and Layé, S. (2016) Endocannabinoid-mediated plasticity in nucleus accumbens controls vulnerability to anxiety after social defeat stress. *Cell Rep.* **16,** 1237–1242 CrossRef Medline
49. Feng, J., Pena, C. J., Purushothaman, I., Engmann, O., Walker, D., Brown, A. N., Issler, O., Doyle, M., Harrigan, E., Mouzon, E., Vialou, V., Shen, L., Dawlaty, M. M., Jaenisch, R., and Nestler, E. J. (2017) Tet1 in nucleus accumbens opposes depression- and anxiety-like behaviors. *Neuropsychopharmacology* **42,** 1657–1669 CrossRef Medline

50. Kim, K. S., Lee, K. W., Baek, I. S., Lim, C. M., Krishnan, V., Lee, J. K., Nestler, E. J., and Han, P. L. (2008) Adenylyl cyclase-5 activity in the nucleus accumbens regulates anxiety-related behavior. *J. Neurochem.* **107,** 105–115 CrossRef Medline
51. Lim, B. K., Huang, K. W., Grueter, B. A., Rothwell, P. E., and Malenka, R. C. (2012) Anhedonia requires MC4R-mediated synaptic adaptations in nucleus accumbens. *Nature* **487,** 183–189 CrossRef Medline
52. Francis, T. C., and Lobo, M. K. (2017) Emerging role for nucleus accumbens medium spiny neuron subtypes in depression. *Biol. Psychiatry* **81,** 645–653 CrossRef Medline
53. Livak, K. J., and Schmittgen, T. D. (2001) Analysis of relative gene expression data using real-time quantitative PCR and the $2(-\Delta\Delta C(T))$ method. *Methods* **25,** 402–408 CrossRef Medline
54. Wang, W., Sun, D., Pan, B., Roberts, C. J., Sun, X., Hillard, C. J., and Liu, Q. S. (2010) Deficiency in endocannabinoid signaling in the nucleus accumbens induced by chronic unpredictable stress. *Neuropsychopharmacology* **35,** 2249–2261 CrossRef Medline
55. Zhu, Z., Wang, G., Ma, K., Cui, S., and Wang, J. H. (2017) GABAergic neurons in nucleus accumbens are correlated to resilience and vulnerability to chronic stress for major depression. *Oncotarget* **8,** 35933–35945 CrossRef Medline
56. Volk, N., Pape, J. C., Engel, M., Zannas, A. S., Cattane, N., Cattaneo, A., Binder, E. B., and Chen, A. (2016) Amygdalar MicroRNA-15a is essential for coping with chronic stress. *Cell Rep.* **17,** 1882–1891 CrossRef Medline
57. Lv, X., Jiang, H., Liu, Y., Lei, X., and Jiao, J. (2014) MicroRNA-15b promotes neurogenesis and inhibits neural progenitor proliferation by directly repressing TET3 during early neocortical development. *EMBO Rep.* **15,** 1305–1314 CrossRef Medline
58. Elferink, L. A., Trimble, W. S., and Scheller, R. H. (1989) Two vesicle-associated membrane protein genes are differentially expressed in the rat central nervous system. *J. Biol. Chem.* **264,** 11061–11064 Medline
59. Pevsner, J., Hsu, S. C., and Scheller, R. H. (1994) n-Sec1: a neural-specific syntaxin-binding protein. *Proc. Natl. Acad. Sci. U.S.A.* **91,** 1445–1449 CrossRef Medline
60. Ravichandran, V., and Roche, P. A. (1997) Cloning and identification of human syntaxin 5 as a synaptobrevin/VAMP binding protein. *J. Mol. Neurosci.* **8,** 159–161 CrossRef Medline
61. Trimble, W. S., Cowan, D. M., and Scheller, R. H. (1988) VAMP-1: a synaptic vesicle-associated integral membrane protein. *Proc. Natl. Acad. Sci. U.S.A.* **85,** 4538–4542 CrossRef Medline
62. Ma, K., Xu, A., Cui, S., Sun, M., Xue, Y., and Wang, J.-H. (2016) Impaired GABA synthesis, uptake and release are associated with depression-like behaviors induced by chronic mild stress. *Transl. Psychiatry* **6,** e910 CrossRef Medline
63. Volk, N., Paul, E. D., Haramati, S., Eitan, C., Fields, B. K., Zwang, R., Gil, S., Lowry, C. A., and Chen, A. (2014) MicroRNA-19b associates with Ago2 in the amygdala following chronic stress and regulates the adrenergic receptor β1. *J. Neurosci.* **34,** 15070–15082 CrossRef Medline
64. Huang, Y. H., Schlüter, O. M., and Dong, Y. (2011) Cocaine-induced homeostatic regulation and dysregulation of nucleus accumbens neurons. *Behav. Brain Res.* **216,** 9–18 CrossRef Medline
65. Wang, X., Luo, Y. X., He, Y. Y., Li, F. Q., Shi, H. S., Xue, L. F., Xue, Y. X., and Lu, L. (2010) Nucleus accumbens core mammalian target of rapamycin signaling pathway is critical for cue-induced reinstatement of cocaine seeking in rats. *J. Neurosci.* **30,** 12632–12641 CrossRef Medline
66. Wang, J. H. (2019) Searching basic units in memory traces: associative memory cells. *F1000Res* **8,** 457 CrossRef Medline
67. Camp, N. J., and Cannon-Albright, L. A. (2005) Dissecting the genetic etiology of major depressive disorder using linkage analysis. *Trends Mol. Med.* **11,** 138–144 CrossRef Medline
68. Klengel, T., and Binder, E. B. (2013) Gene-environment interactions in major depressive disorder. *Can. J. Psychiatry* **58,** 76–83 CrossRef Medline
69. Wilde, A., Mitchell, P. B., Meiser, B., and Schofield, P. R. (2013) Implications of the use of genetic tests in psychiatry, with a focus on major depressive disorder: a review. *Depress Anxiety* **30,** 267–275 CrossRef Medline
70. Manji, H. K., Quiroz, J. A., Sporn, J., Payne, J. L., Denicoff, K., A Gray, N., Zarate C. A., Jr., and Charney, D. S. (2003) Enhancing neuronal plasticity and cellular resilience to develop novel, improved therapeutics for difficult-to-treat depression. *Biol. Psychiatry* 53, 707–742 CrossRef Medline
71. Vialou, V., Robison, A. J., Laplant, Q. C., Covington H. E., 3rd., Dietz, D. M., Ohnishi, Y. N., Mouzon, E., Rush, A. J., 3rd., Watts, E. L., Wallace, D. L., Iñiguez, S. D., Ohnishi, Y. H., Steiner, M. A., Warren, B. L., Krishnan, V., *et al.* (2010) ΔFosB in brain reward circuits mediates resilience to stress and antidepressant responses. *Nat. Neurosci.* **13,** 745–752 CrossRef Medline
72. Nestler, E. J., and Carlezon, W. A., Jr. (2006) The mesolimbic dopamine reward circuit in depression. *Biol. Psychiatry* **59,** 1151–1159 CrossRef Medline
73. Pujara, M., and Koenigs, M. (2014) Mechanisms of reward circuit dysfunction in psychiatric illness: prefrontal–striatal interactions. *Neuroscientist* **20,** 82–95 CrossRef Medline
74. Waraczynski, M. A. (2006) The central extended amygdala network as a proposed circuit underlying reward valuation. *Neurosci. Biobehav. Rev.* **30,** 472–496 CrossRef Medline
75. Bajbouj, M., Lisanby, S. H., Lang, U. E., Danker-Hopfe, H., Heuser, I., and Neu, P. (2006) Evidence for impaired cortical inhibition in patients with unipolar major depression. *Biol. Psychiatry* **59,** 395–400 CrossRef Medline
76. Croarkin, P. E., Levinson, A. J., and Daskalakis, Z. J. (2011) Evidence for GABAergic inhibitory deficits in major depressive disorder. *Neurosci. Biobehav. Rev.* **35,** 818–825 CrossRef Medline
77. Hettema, J. M., An, S. S., Neale, M. C., Bukszar, J., van den Oord, E. J., Kendler, K. S., and Chen, X. (2006) Association between glutamic acid decarboxylase genes and anxiety disorders, major depression, and neuroticism. *Mol. Psychiatry* **11,** 752–762 CrossRef Medline
78. Karolewicz, B., Maciag, D., O'Dwyer, G., Stockmeier, C. A., Feyissa, A. M., and Rajkowska, G. (2010) Reduced level of glutamic acid decarboxylase-67 kDa in the prefrontal cortex in major depression. *Int. J. Neuropsychopharmacol.* **13,** 411–420 CrossRef Medline
79. Khundakar, A., Morris, C., and Thomas, A. J. (2011) The immunohistochemical examination of GABAergic interneuron markers in the dorsolateral prefrontal cortex of patients with late-life depression. *Int. Psychogeriatr.* **23,** 644–653 CrossRef Medline
80. Levinson, A. J., Fitzgerald, P. B., Favalli, G., Blumberger, D. M., Daigle, M., and Daskalakis, Z. J. (2010) Evidence of cortical inhibitory deficits in major depressive disorder. *Biol. Psychiatry* **67,** 458–464 CrossRef Medline
81. Maciag, D., Hughes, J., O'Dwyer, G., Pride, Y., Stockmeier, C. A., Sanacora, G., and Rajkowska, G. (2010) Reduced density of calbindin immunoreactive GABAergic neurons in the occipital cortex in major depression: relevance to neuroimaging studies. *Biol. Psychiatry* **67,** 465–470 CrossRef Medline
82. Oruc, L., Verheyen, G. R., Furac, I., Ivezić, S., Jakovljević, M., Raeymaekers, P., and Van Broeckhoven, C. (1997) Positive association between the GABRA5 gene and unipolar recurrent major depression. *Neuropsychobiology* **36,** 62–64 CrossRef Medline
83. Price, R. B., Shungu, D. C., Mao, X., Nestadt, P., Kelly, C., Collins, K. A., Murrough, J. W., Charney, D. S., and Mathew, S. J. (2009) Amino acid neurotransmitters assessed by proton magnetic resonance spectroscopy: relationship to treatment resistance in major depressive disorder. *Biol. Psychiatry* **65,** 792–800 CrossRef Medline
84. Plante, D. T., Jensen, J. E., Schoerning, L., and Winkelman, J. W. (2012) Reduced γ-aminobutyric acid in occipital and anterior cingulate cortices in primary insomnia: a link to major depressive disorder? *Neuropsychopharmacology* **37,** 1548–1557 CrossRef Medline
85. Rajkowska, G., O'Dwyer, G., Teleki, Z., Stockmeier, C. A., and Miguel-Hidalgo, J. J. (2007) GABAergic neurons immunoreactive for calcium binding proteins are reduced in the prefrontal cortex in major depression. *Neuropsychopharmacology* **32,** 471–482 CrossRef Medline
86. Sanacora, G., Gueorguieva, R., Epperson, C. N., Wu, Y. T., Appel, M., Rothman, D. L., Krystal, J. H., and Mason, G. F. (2004) Subtype-specific alterations of γ-aminobutyric acid and glutamate in patients with major depression. *Arch. Gen. Psychiatry* **61,** 705–713 CrossRef Medline

87. Torrey, E. F., Barci, B. M., Webster, M. J., Bartko, J. J., Meador-Woodruff, J. H., and Knable, M. B. (2005) Neurochemical markers for schizophrenia, bipolar disorder, and major depression in postmortem brains. *Biol. Psychiatry* **57,** 252–260 CrossRef Medline
88. Xu, A., Cui, S., and Wang, J. (2016) Incoordination among subcellular compartments is associated to depression-like behavior induced by chronic mild stress. *Int. J. Neuropsychopharmacol.* **19,** pyv122 CrossRef Medline
89. Veeraiah, P., Noronha, J. M., Maitra, S., Bagga, P., Khandelwal, N., Chakravarty, S., Kumar, A., and Patel, A. B. (2014) Dysfunctional glutamatergic and γ-aminobutyric acidergic activities in prefrontal cortex of mice in social defeat model of depression. *Biol. Psychiatry* **76,** 231–238 CrossRef Medline
90. Zhang, G., Gao, Z., Guan, S., Zhu, Y., and Wang, J. H. (2013) Upregulation of excitatory neurons and downregulation of inhibitory neurons in barrel cortex are associated with loss of whisker inputs. *Mol. Brain* **6,** 2 CrossRef Medline
91. Golden, S. A., Covington H. E., 3rd., Berton, O., and Russo, S. J. (2011) A standardized protocol for repeated social defeat stress in mice. *Nat. Protoc.* **6,** 1183–1191 CrossRef Medline
92. Hammels, C., Pishva, E., De Vry, J., van den Hove, D. L., Prickaerts, J., van Winkel, R., Selten, J. P., Lesch, K. P., Daskalakis, N. P., Steinbusch, H. W., van Os, J., Kenis, G., and Rutten, B. P. (2015) Defeat stress in rodents: From behavior to molecules. *Neurosci. Biobehav. Rev.* **59,** 111–140 CrossRef Medline
93. Sun, Y., Lu, W., Du, K., and Wang, J. H. (2019) microRNA and mRNA profiles in the amygdala are relevant to fear memory induced by physical or psychological stress. *J. Neurophysiol.* **122,** 1002–1022 CrossRef Medline
94. Wang, J. H., and Cui, S. (2017) Associative memory cells: formation, function and perspective. *F1000Res* **6,** 283 CrossRef Medline
95. Wang, J. H., and Cui, S. (2018) Associative memory cells and their working principle in the brain. *F1000Res* **7,** 108 CrossRef Medline
96. Dellu, F., Mayo, W., Cherkaoui, J., Le Moal, M., and Simon, H. (1992) A two-trial memory task with automated recording: study in young and aged rats. *Brain Res.* **588,** 132–139 CrossRef Medline
97. Overstreet, D. H. (2012) Modeling depression in animal models. *Methods Mol. Biol.* **829,** 125–144 CrossRef Medline
98. Krützfeldt, J., Rajewsky, N., Braich, R., Rajeev, K. G., Tuschl, T., Manoharan, M., and Stoffel, M. (2005) Silencing of microRNAs *in vivo* with 'antagomirs'. *Nature* **438,** 685–689 CrossRef Medline
99. Chen, N., Chen, X., and Wang, J.-H. (2008) Homeostasis established by coordination of subcellular compartment plasticity improves spike encoding. *J. Cell Sci.* **121,** 2961–2971 CrossRef Medline
100. Ge, R., Qian, H., Chen, N., and Wang, J. H. (2014) Input-dependent subcellular localization of spike initiation between soma and axon at cortical pyramidal neurons. *Mol. Brain* **7,** 26 CrossRef Medline
101. Wang, J.-H., and Kelly, P. (2001) Ca^{2+}/CaM signalling pathway up-regulates glutamatergic synaptic function in non-pyramidal fast-spiking neurons of hippocampal CA1. *J. Physiol.* **533,** 407–422 CrossRef Medline
102. Freund, T. F., and Buzsáki, G. (1996) Interneurons of the hippocampus. *Hippocampus* **6,** 347–470 CrossRef Medline
103. Lu, W., Wen, B., Zhang, F., and Wang, J. H. (2014) Voltage-independent sodium channels emerge for an expression of activity-induced spontaneous spikes in GABAergic neurons. *Mol. Brain* **7,** 38 CrossRef Medline
104. McKay, B. E., and Turner, R. W. (2005) Physiological and morphological development of the rat cerebellar Purkinje cell. *J. Physiol.* **567,** 829–850 CrossRef Medline
105. Wang, J. H., Wei, J., Chen, X., Yu, J., Chen, N., and Shi, J. (2008) The gain and fidelity of transmission patterns at cortical excitatory unitary synapses improve spike encoding. *J. Cell Sci.* **121,** 2951–2960 CrossRef Medline
106. Yang, Z., Chen, N., Ge, R., Qian, H., and Wang, J.-H. (2017) Functional compatibility between Purkinje cell axon branches and their target neurons in the cerebellum. *Oncotarget* **8,** 72424–72437 CrossRef Medline
107. Ge, R., Qian, H., and Wang, J. H. (2011) Physiological synaptic signals initiate sequential spikes at soma of cortical pyramidal neurons. *Mol. Brain* **4,** 19 CrossRef Medline
108. Yan, F., Gao, Z., Chen, P., Huang, L., Wang, D., Chen, N., Wu, R., Feng, J., Cui, S., Lu, W., and Wang, J.-H. (2016) Coordinated plasticity between barrel cortical glutamatergic and GABAergic neurons during associative memory. *Neural Plast.* **2016,** 5648390 CrossRef Medline
109. Yang, Z., Gu, E., Lu, X., and Wang, J. H. (2014) Essential role of axonal VGSC inactivation in time-dependent deceleration and unreliability of spike propagation at cerebellar Purkinje cells. *Mol. Brain* **7,** 1 CrossRef Medline
110. Wang, J.-H. (2003) Short-term cerebral ischemia causes the dysfunction of interneurons and more excitation of pyramidal neurons. *Brain Res. Bull.* **60,** 53–58 CrossRef Medline
111. Yu, J., Qian, H., and Wang, J. H. (2012) Upregulation of transmitter release probability improves a conversion of synaptic analogue signals into neuronal digital spikes. *Mol. Brain* **5,** 26 CrossRef Medline
112. Wei, J., Zhang, M., Zhu, Y., and Wang, J. H. (2004) Ca^{2+}-calmodulin signalling pathway upregulates GABA synaptic transmission through cytoskeleton-mediated mechanisms. *Neuroscience* **127,** 637–647 CrossRef Medline
113. Zhang, F., Liu, B., Lei, Z., and Wang, J. (2012) mGluR1,5 activation improves network asynchrony and GABAergic synapse attenuation in the amygdala: implication for anxiety-like behavior in DBA/2 mice. *Mol. Brain* **5,** 20 CrossRef Medline
114. Xu, W., and Südhof, T. C. (2013) A neural circuit for memory specificity and generalization. *Science* **339,** 1290–1295 CrossRef Medline
115. Paxinos, G., and Watson, C. (2005) *The Mouse Brain: In Stereotaxic Coordinates* (Paxinos, G. and Watson, C., eds), pp. 1–350, Elsevier Academic Press, Orlando
116. Feng, J., Lu, W., Wang, D., Ma, K., Song, Z., Chen, N., Sun, Y., Du, K., Shen, M., Cui, S., and Wang, J.-H. (2017) Barrel cortical neuron integrates triple associated signals for their memory through receiving epigenetic-mediated new synapse innervations. *Cereb. Cortex* **27,** 5858–5871 CrossRef Medline
117. Gao, Z., Wu, R., Chen, C., Wen, B., Liu, Y., Lu, W., Chen, N., Feng, J., Fan, R., Wang, D., Cui, S., and Wang, J. H. (2019) Coactivations of barrel and piriform cortices induce their mutual synapse innervations and recruit associative memory cells. *Brain Res.* **1721,** 146333 CrossRef Medline
118. Lei, Z., Wang, D., Chen, N., Ma, K., Lu, W., Song, Z., Cui, S., and Wang, J.-H. (2017) Synapse innervation and associative memory cell are recruited for integrative storage of whisker and odor signals in the barrel cortex through miRNA-mediated processes. *Front. Cell. Neurosci.* **11,** 316 CrossRef Medline
119. Gao, Z., Chen, L., Fan, R., Lu, W., Wang, D., Cui, S., Huang, L., Zhao, S., Guan, S., Zhu, Y., and Wang, J.-H. (2016) Associations of unilateral whisker and olfactory signals induce synapse formation and memory cell recruitment in bilateral barrel cortices: cellular mechanism for unilateral training toward bilateral memory. *Front. Cell. Neurosci.* **10,** 285 CrossRef Medline
120. Hama, H., Kurokawa, H., Kawano, H., Ando, R., Shimogori, T., Noda, H., Fukami, K., Sakaue-Sawano, A., and Miyawaki, A. (2011) Scale: a chemical approach for fluorescence imaging and reconstruction of transparent mouse brain. *Nat. Neurosci.* **14,** 1481–1488 CrossRef Medline